

INTRODUCTION

1 The Structure of Adenoviruses.

Adenoviruses belong to the family of *Adenoviridae*, their genome is a linear, double stranded DNA of about 36 kb surrounded by a protein structure with an icosahedral shape named capsid. They are able to infect a wide host range of post-mitotic cells, even those in highly differentiated tissues such as skeletal muscle, lung, brain and heart. The Adenoviruses were first discovered more than 50 years ago by Rowe and colleagues from human adenoid cells (Rowe et al., 1953). Since then, more than 100 different species have been identified from various species including chimpanzees, pig, mouse, dog and birds and all of them are characterized by a distinctive architecture and a common chemical composition. Human adenoviruses cause diseases ranging from respiratory infections and conjunctivitis to gastrointestinal problem. Based on their sequence homology and ability to agglutinate red blood cells, they are classified into 6 subgroups (A-F), which are further subdivided into 51 serotypes (Lukashok, 1998). Among human adenoviruses, serotype 2 (Ad2) and serotype 5 (Ad5) of subgroup C are the most extensively studied. The adenoviral virion was morphologically characterized for the first time in 1993 (Stewart, 1993). It is a nonenveloped particle about 70-90 nm in size with an outer protein shell (capsid) surrounding an inner nucleoprotein core (*Fig. 1*). The icosahedral capsid consists of 252 capsomers divided in 240 hexons and 12 pentons. Each hexon is composed of three monomeric polypeptides (polypeptide II) forming the 20 triangular facets of the capsid; the penton, instead, shows a more complex structure, constituted by five monomeric polypeptides (polypeptide III), which act to anchor a trimeric protein, the fiber (polypeptide IV). The penton and the fiber form the penton complex that seals the capsid at each of the 12 virion vertices. These proteins are responsible for the attachment (fiber) and internalization (penton) of the virus into host cells. The only penton has properties like a toxin: the purified protein provokes a cytopathic effect even without the other viral proteins. The capsid is composed also of a number of other minor components including protein IIIa, pVI, pVIII and pIX. Adenovirus cores contain the viral genome, a linear, double stranded DNA that is approximately 36 kb long. Each end of the genome has an inverted terminal repeat (ITR) of 100-140

bp with a terminal protein (TP) attached covalently (Rekosh, 1977). This protein protects the DNA from the endonucleases of the host cell. The genome is associated with other proteins like the basic protein VII and a small peptide termed *mu* (Anderson, 1989), with the function to stabilize the DNA into the capsid. Another protein is packaged with the DNA, the protein V. This protein is attached to the genome on one side and on the other side to the capsid protein VI, so it links the viral DNA to the capsid (Matthews, 1994). The virions contain also some copies of the adenovirus protease (Pr), that cleaves many of the structural preproteins into their mature forms during the last stage of viral assembly (Webster, 1989).

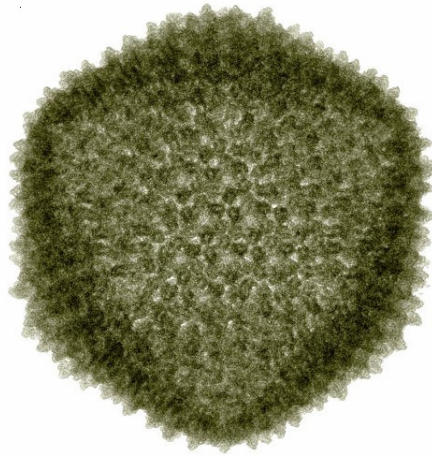
2 Viral life cycle.

2.1 Early events in adenovirus infection.

The adenovirus infection can be divided into two phases. The first is named “early” phase and occurs in 6-8 hours. This phase comprises the entry of the virus into the host cell, the passage of the viral genome into the cytoplasm to the nucleus, the internalization of the adenoviral DNA into the nucleus and the transcription and translation of some viral genes, named early genes. These events modulate the cell metabolism to facilitate the replication of the virus DNA. The second phase is the “late” phase which can take about 4-6 hours after the beginning of the transcription of the late genes.

The initial attachment of the virion particles to the cell surface occurs through an high affinity binding between a portion of the fiber (*knob* domain) and a cell receptor. The first receptor identified was shown to be identical to that for Coxsackie B virus and has therefore been termed coxsackie/adenovirus receptor (CAR) (Bergelson, 1997). CAR is a type I transmembrane protein of 46 kDa belonging to the immunoglobulin superfamily which is present on the basolateral membrane of several epithelial cells in many tissues including heart, lung, liver

A



B

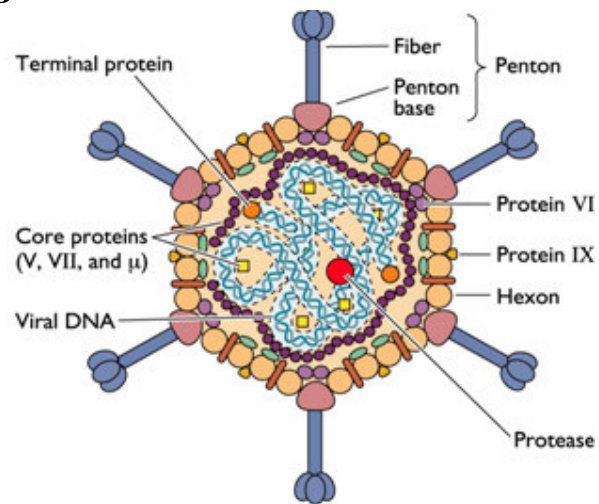
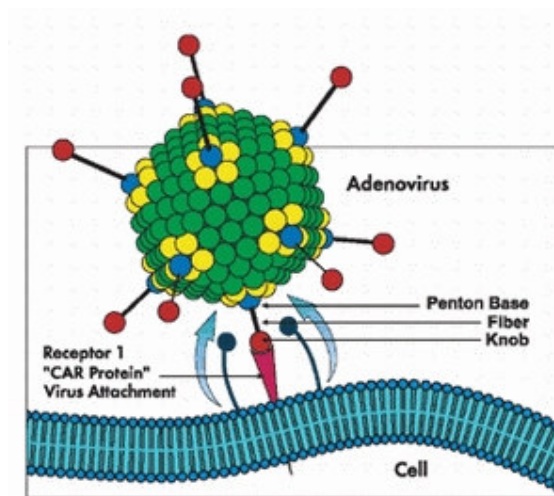


Figure 1. Adenovirus structure.

(**A**) A three-dimensional cryo-EM image reconstruction of Ad5 viewed along the 3-fold axis of the icosahedral capsid (**B**) A stylized section of the adenovirus virion, indicating the relative orientations of the protein components and the viral DNA.

and brain (**Fig. 2A**). All groups of adenoviruses use CAR for the adsorption of the virus to the target cell, except the adenoviruses of group B. These viruses bind another cellular receptor, the CD46, a complement regulatory protein (Gaggar, 2003). Therefore, the adenoviruses of group B are capable to infect some cells, like hematopoietic stem cells, dendritic cells and malignant tumor cells, which are resistant to the infection by the adenoviruses using CAR as the primary attachment receptor. All these data suggest that receptor recognition could be a key factor involved in cell tropism, to the point to change it. The adenovirus fiber can be modified by constructing chimeric viruses carrying fiber genes from different serotypes, or by binding the fiber with several antibodies (Balamotis, 2004; Cerullo, 2007). After the initial attachment of the fiber *knob* portion to the cell surface, an RGD motif, exposed on the penton base (Stewart, 1997), interacts with cellular α_v integrins (Wickham, 1993), in presence of divalent cations. In particular, the heterodimeric integrins, $\alpha_v\beta_3$ and $\alpha_v\beta_5$, support the adenovirus internalization playing an important role in the determination of the tropism (**Fig. 2B**). The interaction between adenovirus and plasma membrane can induce the activation of several signaling pathways like that of phosphoinositide-3-OH kinase (PI-3K), which triggers the Rho family of GTPases with consequential polymerization of actin and cytoskeletal reorganization (Li, 1998). Another pathway, activated 20 minutes post infection, is the Raf/Mitogen-activated protein kinase (MAPK) pathway, which culminates in the production of interleuchin 8 (IL-8) (Bruder, 1997). Together, these events induce the adenovirus internalization through a clathrin-mediated endocytosis. In the acidic environment of the endosome, the virus-encoded protease mediates the dismemberment of the viral capsid through the proteolysis of the protein VI, which induces, in turn, the escape of virions to the cytoplasm. The passage through the cytoplasm to the nucleus seems to be mediated by the cellular protein p32 (Matthews, 1998), which binds the virus core (constituted by the DNA and its associated proteins TP, *mu*, proteins VII and V), and involves dynein and microtubules (Leopold, 2000). One hour after the infection, it is possible to detect the virion on the nuclear membrane. Once inside the nucleus, the viral genome is targeted to the nuclear

A



B

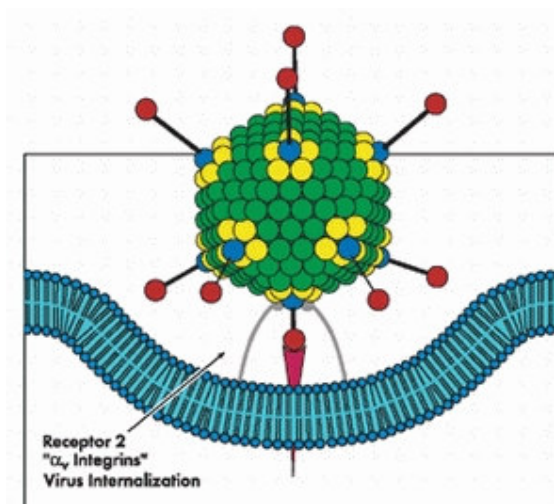


Figure 2. Adenovirus interaction with cell surface.

(A) Schematic representation of adenoviral fiber with the cell receptor, CAR. (B) The second adenoviral interaction between the penton and the α_v integrins to allow virus internalization.

matrix, where TP forms a complex with the cellular CAD pyrimidine synthesis enzyme (Angeletti, 1998) and p32 binds the nuclear lamin B to permit the dissociation between the viral DNA and the linked proteins.

2.2 Early gene and DNA replication.

The transcription of adenoviral genes can be divided in two phases, early and late, respectively occurring before or after viral DNA replication (*Fig. 3*). The first viral transcribed gene is E1, which encodes for two products: E1A and E1B, each of them producing multiple proteins by way of differential mRNA processing. Two E1A transcripts are produced during early infection, encoding the 289R protein and 243R protein. These proteins have the function to modulate the cellular metabolism to make the cell more susceptible to virus replication. In order to do this, they act as *trans*-activators on the other early adenovirus genes and induce the cells to enter in S phase (Berk, 1986). Indeed, both 289R and 243R protein are able to sequester Rb protein (Retinoblastoma protein), bounded to the transcriptional factor E2F, allowing the release of this factor and the activation of its target genes necessary for driving the cell into S phase (Harlow, 1986). Moreover, E1A proteins can also bind proteins involved in the control of cell cycle, such as cyclin-dependent-kinase-inhibitor p21, or factors mediating chromatin structure like p400, pCAF and p300/CBP. The E1B gene product 55K (E1B-55K) acts blocking p53-dependent apoptosis by directly binding p53, accumulated during cell cycle deregulation by E1A, and inhibiting its ability to induce expression of proapoptotic genes (Ben-Israel, 2002). Instead, the other product of E1B gene, E1B-19K, blocks the pathway of programmed cell death binding directly the proapoptotic proteins Bak and Bax (Sundararajan, 2001). These mechanisms keep the cell alive as long as possible in order to permit the virus replication.

The E2 gene products (E2A and E2B) are proteins that are necessary for the replication of viral genome and the ensuring transcription of late genes. The

latters are a DNA polymerase, the preterminal protein (pTP) and the 72-kDa single stranded DNA binding protein (DBP).

The E3 gene expression is indispensable for subverting the host defence mechanism, allowing the persistence of infected cells. Indeed, the E3-gp19K can interfere with the presentation of the viral antigen, preventing the translocation of MHC class I (major histocompatibility complex) molecules to the cell surface by sequestering them in the endoplasmic reticulum (Bennett, 1999). Moreover, the E3-10.4K, 14.5K and 14.7K proteins inhibit the apoptotic pathway inducing the clearance of TNF- α , Fas ligand (FasL) and TRAIL receptors from the cell membrane.

The gene products derived from the E4 cassette are involved in cell cycle control (E4orf6 cooperates with the E1B-55K protein in the sequestration of p53), promote virus replication and shut-off the host protein synthesis (Querido, 2001). During the last steps of early phase of the adenovirus infection, the viral DNA replication begins but requires sequences within the ITRs as origin of replication. Moreover, because the viral genome does not have telomeres, the integrity of DNA ends is ensured by the viral protein pTP. This protein is covalently linked to the 5' end of each genome strand and acts as a primer for the viral DNA polymerase. The genes are encoded on both strands of DNA in a series of overlapping transcription units.

2.3 Late gene expression and viral assembly.

After viral DNA replication, the transcription of late genes begins (*Fig. 3*). A key role in the control of this phase is played by the major late promoter (MLP), which is attenuated during the early stage of infection. In fact, during the “early phase”, the basal level of transcription is low while, after the viral DNA replication and the high expression of IVa2 and IX genes, the transcription via the MLP is fully functional. From the MLP, 5 genes (L1-L5) are transcribed as single pre-mRNAs, each one encoding from 15 to 20 different mRNAs by differential splicing and polyadenylation. These transcripts encode structural proteins and other proteins involved in virion assembly.

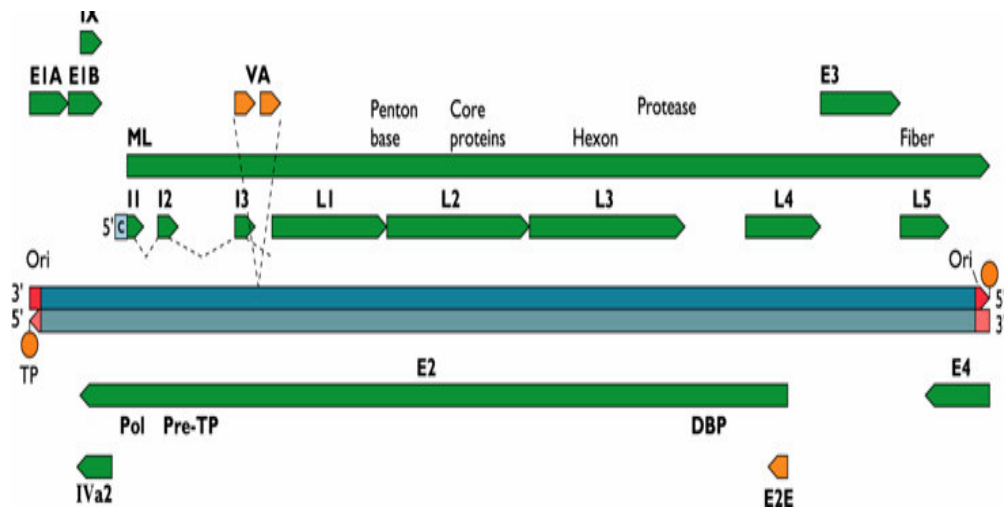


Figure 3. Schematic representation of genome and transcription units.

The central, solid line represents the viral genome. Positions of the left and right ITRs, the early transcription units (E1A, E1B, E2, E3, and E4), and the major late transcription unit (major late promoter (ML), L1–L5) are shown. Arrows indicate the direction of transcription.

The virion assembly takes place in the nucleus, but the hexon trimerization begins in the cytoplasm and, subsequently, the hexon trimers move to the nucleus where they are associated with pentons and minor proteins to form the capsid (Cepko, 1983). The viral genome encapsidation requires the L1-52/55K, IVa2, L4-33K proteins (Hasson, 1989; Zhang, 2003; Fessler, 1999) and the packaging signal, which consists in a series of seven repeats (A1-A7), enriched in AT, at the left end of the adenoviral DNA. These events are accompanied by changes in the nuclear structure. About 30 hours after infection, the host cell is lysed in a process involving the ADP protein (adenovirus death protein), a product of E3 gene, which is expressed only during the late phase of infection and is transcribed from MLP rather than E3 promoter (Tollefson, 1996).

3 Adenoviruses as vectors.

3.1 First and second generation of adenoviral vectors.

The adenoviruses can be used in the gene therapy field as vectors carrying the therapeutic gene into target cells, where the same gene is defective. In fact, it is possible to take advantage by the natural ability of virus to infect and deliver their genes to human cells in a pathogenic manner. Handling their genome, it has been possible to obtain several adenoviral vectors: first generation vectors (FG-Ad), second generation vectors and helper dependent vectors (HD-Ad).

In the first generation vectors, the E1 and/or E3 genes cassette are removed, resulting in viruses that are impaired in their ability to replicate (replication deficient adenoviral vectors, RDA) (*Fig. 4*). These vectors retain the ITRs, the packaging signal and the other genes whereas the E1/E3 cassettes are replaced by a transgene of 6-8 kb long, often under the control of a heterologous promoter. The production strategy of FG-Ad vectors consists in the generation of the adenoviral genome by homologous recombination between a backbone plasmid (pAdEasy), expressing all adenovirus genes except E1 and/or E3, and a plasmid shuttling the gene of interest (He, 1998) (*Fig. 5*). When vector genome is obtained, its large scale production is possible using the HEK-293 cell line, a

human embryonic kidney-derived cell line, that provide the E1 functions *in trans* (Graham, 1977). Although the FG-Ad vectors exhibit many advantages, as their ability to infect post-mitotic cells in highly differentiated tissues, liver tropism after systemic administration and high titer production (1×10^{13} vp/ml), some troubles exist with their use. In fact, during the vector production, a recombination between the E1 region sequences in the packaging cells (HEK-293) and the recombinant virus can give rise to viral progeny with functional E1 genes, that are replication competent adenovirus (RCA) (Lochmuller, 1994). The second and more troublesome problem associated with the use of FG-Ad vectors consists in their stimulation of the host immune response. This response is due to low levels of vector replication, that can occur even in the absence of the E1 genes (Yang, 1994), resulting in the destruction of transduced cells and in the low persistence of transgene. In order to prevent these problems, a second generation (SG-Ad) vectors has been produced (**Fig. 4**). These vectors are characterised by deletion of E2 and/or E4 coding sequences, providing both the benefits of a less probability of recombination to give RCA and a larger capacity for the transgene insertion. Nevertheless, the inhibition of viral gene expression by E1 gene is not much efficient. For this reason, the host immune response is a major impediment in using these vectors for applications requiring long-term gene expression.

3.2 Helper-dependent vectors.

To improve the safety and efficiency of Ad-based vectors, other vectors have been constructed: the helper-dependent adenoviral vectors (HD-Ad). These vectors are deleted of all viral coding sequences (hence they are called also gutless) while only the two ITRs and the packaging signal is left. Because efficient packaging into the Ad capsid requires a genome size between 28 kb and 38 kb, stuffer DNA is introduced in HD-Ads. The nature of this stuffer DNA is noncoding mammalian DNA with minimal repeat sequences. Moreover, because HD-Ad vectors are deleted of all viral coding sequences, all proteins for vector replication and assembly are required *in trans*. Accordingly, for their propagation these vectors need a virus helper, a particular FG-Ad vector bearing packaging signal

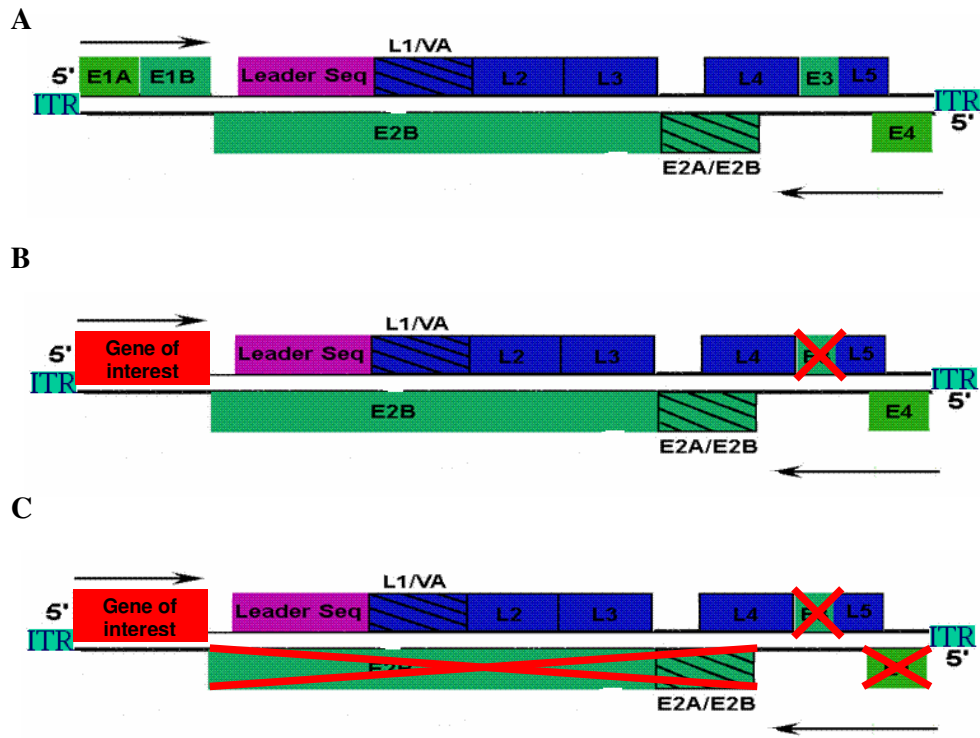


Figure 4. Schematic representation of adenoviral vectors.

(A) Adenovirus genome. (B) First generation adenoviral vectors. (C) Second generation adenoviral vectors.

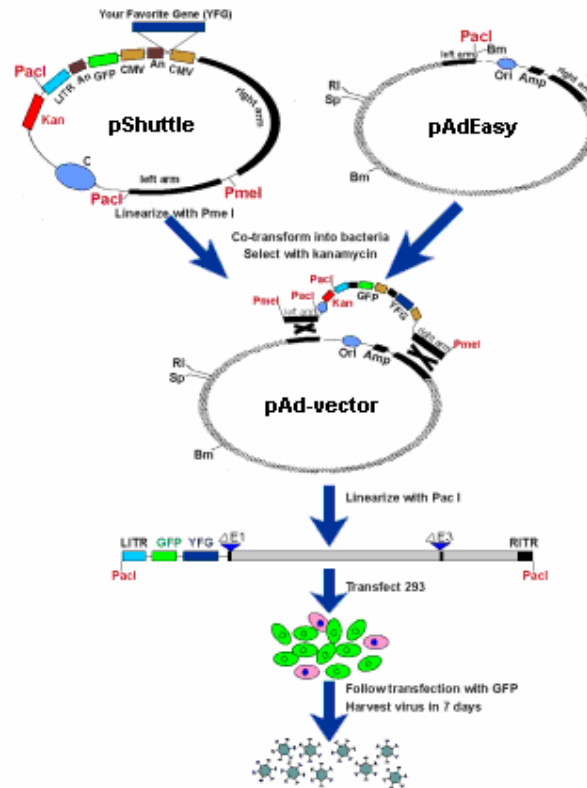


Figure 5. Schematic representation of First generation adenoviral vectors production.

A plasmid expressing the transgene of interest (pShuttle) is recombined with a backbone plasmid (pAdEasy), expressing all adenovirus genes except E1 and/or E3. After the homologous recombination, the pAd vector is linearized and transfected in 293 cells to proceed with the large scale production of vector.

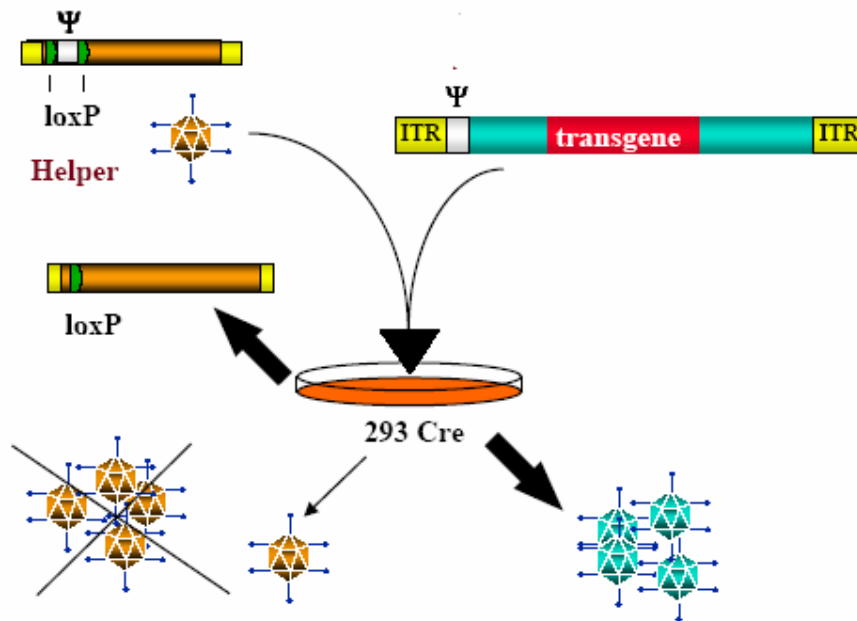


Figure 6. Schematic representation of Helper dependent adenoviral vectors production.

A plasmid expressing the transgene of interest is transfected in 293 Cre cells and subsequently the cells are infected with a virus Helper. The Cre recombinase mediates site specific recombination between loxP sites, that flanked the packaging signal of the Helper virus, rendering the helper viral genome unpackageable but still able to *trans*-complement the replication and the encapsidation of the HD-Ad genome

flanked by loxP sites, the target sequences for the recombinase Cre (Parks, 1996) (**Fig. 6**). The packaging cell line 293Cre are transfected with linearized HD-Ad genome and subsequently infected with the helper virus. After the infection, the packaging signal of the helper virus is excised by Cre-mediated site specific recombination between loxP sites, rendering the helper viral genome unpackageable but still able to *trans*-complement the replication and the encapsidation of the HD-Ad genome. The large scale production of a HD-Ad vector is carried out by several coinfections of 293Cre cells with HD-Ad and the helper virus. Finally, the HD-Ad vector is purified on CsCl gradient ultracentrifugation. To obtain large quantities of HD-Ad vectors with a low helper virus contamination (a necessary condition for *in vivo* approaches) the Cre-loxP method is improved by Ng (Palmer, 2003). The new strategy of production consists in the use of a suspension-adapted cell line (116Cre) expressing higher levels of Cre than 293Cre cells. The helper virus should have a longer DNA insertion into the E3 region, such to render its genome large enough to permit a physical separation from HD-Ad after the CsCl purification. Moreover, the helper virus presents the packaging signal in an orientation opposite to that of HD-Ads, so that the possibility of homologous recombination between these two elements is reduced and, in turn, also the generation of RCAs. These improvements allow to produce, in about two weeks, more than 1×10^{13} viral particles per ml (vp/ml) starting from 3 liters of cells ($3-4 \times 10^8$ total cells), with a helper virus contamination, after CsCl purification, of about 0,02 - 0,01%, as determined by DNA-based assay.

The HD-Ad vectors retain several advantages of FA-Ads, including a high efficiency of *in vivo* liver transduction, after their systemic administration, and a high level of transgene expression. Moreover, the deletion of the viral genes permits a large cloning capacity of about 37 kb, allowing the insertion of whole or multiple genes and large *cis*-acting elements to enhance, prolong and regulate transgene expression (Morrall, 1998). The absence of viral genes in transduced cells makes the HD-Ad vectors able to mediate high levels, long term transgene expression in absence of chronic toxicity (Schiedner, 1998). However, some aspects of toxicity persist also with the use of HD-Ad vectors.

3.3 Immune response to Ad based vectors.

Although the HD-Ad vectors are compelling candidates for gene therapy application, the immune response to the vector is a major impediment to their use in clinical, because it leads to the elimination of the vector and the transfected cells, decreasing both the intensity and the duration of transgenic protein expression. In addition, the memory response would then thwart further efforts to use the same vector or transgene. However, when the goal is vaccination or tumor lysis, this response may be beneficial.

The immune response induced by intravenous delivery of Ad vectors revealed a biphasic response comprised of an early or acute phase and a late or chronic phase (*Fig. 7*). The former is due to the activation of the innate immune system, mainly consisting of a rapid (few hours) inflammatory cytokines and chemokines secretion; the latter is the adaptive immunity, leading to antibodies production and T lymphocytes activation in a few days after vectors administration. These two phases are induced by different portions of Ad: the expression of proinflammatory mediators occurs before substantial viral gene transcription, suggesting that the adenoviral capsid triggers this response (it is induced by FG-Ad, HD-Ad vectors and ultraviolet/psoralen inactivated Ad vectors) (Liu, 2003; Muruve 2003); on the other hand, the adaptive response is not observed after the administration of HD-Ad and inactivated vectors, confirming that viral gene transcription is required for this response.

Immediately after the injection of Ad vectors, the Ad particles interact with cells and proteins in the blood. The interaction with neutrophils, macrophages, dendritic cells, NK cells and complement lead to initiate and sustain the cascade of proinflammatory cytokines. In particular, granulocytes such as neutrophils, represent the main source of cytokines; NK cells are interferon α/β responsive cells that perform cytolytic functions; NK and T cells, via IL-12 and IL-18, secrete interferon γ that is essential in the development of helper T cell type 1 (Th1). Finally, monocytes/macrophages are phagocytes that not only secrete antiviral cytokines but also present the antigen required for adaptive immunity. Moreover, the interaction with C3 complement leads to activation of neutrophils

and rapid release of the chemokines, which further recruits and activates inflammatory cell infiltrate to the circulatory system (Cotter, 2005; Kiang, 2006). Ad also interacts directly with CAR receptor present on platelet cell surface, causing platelets activation with increased levels of D-dimer and up-regulation of adhesion molecules like ICAM-1 and VCAM-1 (Othman, 2007; Baker, 2007). These molecules allow an increased adhesion and migration of infiltrating leukocytes, and extensive platelet/leukocyte aggregation, leading to clearance of activated platelets by scavenger macrophages. For this reason, the most consistent markers of immune activation are the increased levels of systemic cytokines (IL-6, IL-12, TNF- α , RANTES, MCP-1, IFN- α) and thrombocytopenia. Within 24 hours, the innate response eliminates about 80% of adenoviral particles. At molecular level, different pathways recognize viral pathogens and induce secretion of cytokines (*Fig. 8*). The first type of viral innate immune response sensor belongs to RNA helicase family and includes RIG-1 and MDA-5, which are ubiquitously expressed in the cytosol. The recognition of RNA by these helicases results in the recruitment of the adaptor protein MAVS, which stimulates the TANK-related kinases TBK1 and IKK ϵ , leading to the phosphorylation of IRF3 and IRF7, the main transcription factors of type I interferons. A similar signalling network is crucial in sensing Ad infections, leading to activation of IRF3, through specific cytosolic sensor of foreign DNA (Nociari, 2007). Another set of molecular sensors includes the family of pattern recognition receptors called Toll-like receptors (TLR), which are expressed primarily on the cell membrane or in the endosomal compartment of macrophages and DC. They are single spanning transmembrane proteins that can be in homodimeric or heterodimeric form, suggesting that the diversity of their pattern of recognition may be increased by combinatorial interactions (Akira, 2006). However, TLR3, TLR7/8 and TLR9 recognize dsRNA, ssRNA and dsDNA respectively; TLR4 mediates the recognition of LPS; TLR2 is important for the response to cytomegalovirus and measles virus. Engagement of a TLR family member initiates a network of signalling cascades, involving the intracellular adaptor proteins MyD88 and/or TRIF. In particular, MyD88 activates the proteins of IRAK family and TRAF6, leading the activation of TAK1, which in turn

activates the I κ B kinases. So, the transcription factor NF κ B translocates to the nucleus and induces the expression of several cytokines. Another consequence of IRAK signalling is the phosphorylation and activation of the transcription factors IRF3 and IRF7, which also induce and/or regulate secretion of inflammatory cytokines (Kaisho, 2006). Recently, it has been shown that TLR9 is a sensor of dsDNA of HD-Ad backbone in primary macrophages, a finding which is consistent with its localization in the endosomal compartment, where capsid dissociation is thought to occur. Moreover, the TLR9 mRNA is upregulated during the early phase of viral infection, suggesting that it may predispose APCs to sensing the invading pathogen (Cerullo, 2007). At the moment, it is unknown whether a putative “surface sensor” of the viral capsid may work together with the intracellular sensors. However, the innate immune response to adenoviral vectors is dose dependent: a higher dose of the adenoviral vector induces a stronger inflammatory response, which accounts for the elimination of infected cells and leads to a decrease in transgene expression. This plateau effect is probably attributable to saturation of adenovirus receptors such as CAR.

Four-five days after the intravenous administration of Ad vectors, the adaptive immune response is activated. It consists of two components: a cellular immune and a humoral response (**Fig. 9**). In general, the former is activated by antigen presenting cells (APCs) that, after the uptake of the Ad, process the viral proteins and present them at the major histocompatibility complex (MHC) class I, on the cell surface (Kafri, 1998). Once the MHC-I is loaded with viral proteins, it binds to the CD8⁺ T cells and, in the presence of a co-stimulatory signal (the interaction between CD28 and B7), activates them in order to form cytotoxic T lymphocytes (CTL) which finally destroy the transduced cells. The cellular immune response is further stimulated by CD4⁺ cells, belonging to the Th1 subset. These cells are activated by epitopes presented by MHC class II molecules at the surface of APCs, whose activation triggers the secretion of IL-2 and INF- γ . These cytokines, in turn, induce the differentiation of CD8⁺ T cells into CTLs and the up regulation of MHC-I expression in Ad transduced cells, consequently facilitating their recognition by CTLs. Apart from the cellular immune response, the adaptive immune system also induces a humoral response that is initiated by the binding of

Ad particles to the surface immunoglobulin of B cells. After internalization and processing of the virus, the Ad epitopes are presented at the surface of B cells by MHC II molecules where they are recognized by activated T helper cells of the Th2 subset. These specific CD4+ cells release cytokines like IL-4, IL-5, IL-6 and IL-10, which provide signals for the B cells to differentiate into plasma cells. The plasma cells secrete antibodies (Abs) directed towards the adenoviral capsid, preventing the Ad cell entry and promoting the opsonisation by macrophages. Consequently, these Abs hamper the efficiency of repeated administration of adenoviral vectors.

The HD-Ad vectors induce a weaker T cell response, compared to FG-Ads, because of the deletion of adenoviral genes. However, even in the absence of viral transcription, a cytotoxic T cell response can be induced by these vectors. This response may be ascribable to the immunogenicity of adenoviral capsid proteins, that also promote the innate response. Hiding the viral capsid, it could be possible to escape the host immune response.

3.4 PEGylation and preliminary data.

Adenoviral vectors are promising candidates for *in vivo* delivery of several therapeutic genes, but their systemic administration leads to the activation of innate and antigen specific immunity. Different strategies have been proposed to block the immune response, such as the induction of tolerance by oral administration of the virus (Ilan, 1999) or the administration of viruses to neonatal animals (Walter, 1996). However, in both cases, complicated treatment protocols should be required and, moreover, these should not be viable treatments in case of therapy of patients with severe pathological diseases. Successful results in modulating the immune response against Ad vectors have been obtained using pharmacological regimens designed to produce a general immunosuppression, including treatment with cyclophosphamide (Kuriyama, 1999), FK506 and cyclosporine A (Fang, 1995). Although these agents reduce the formation of neutralizing antibodies against viral capsid proteins, they can produce significant untoward side effects and impair pre-existing immunity to other pathogens. For

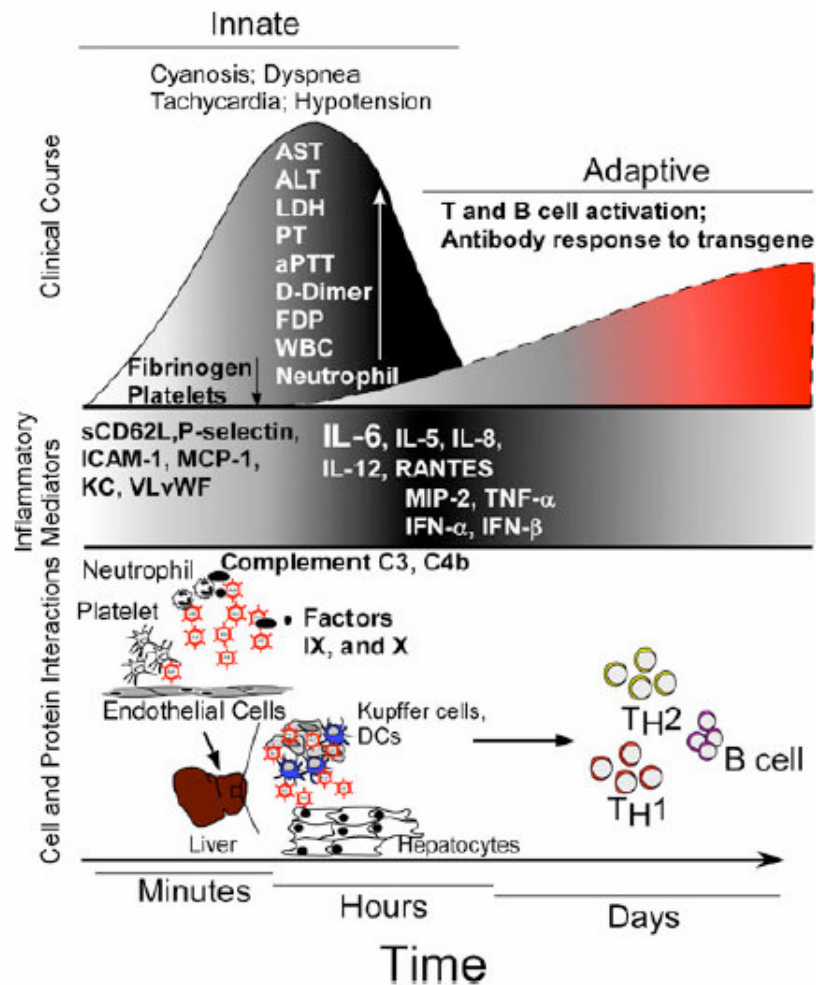


Figure 7. Representation of immune response to adenoviral vectors.

Complex bloodborne protein and cellular factors interact with HDV within minutes of systemic administration (bottom). The cascade of inflammatory mediators initiated by the immediate cellular interactions (middle) exacerbates the clinical manifestations shown (top) over several hours. The induction of innate immune responses initiated days earlier, leads to activation of antigen presenting cells and subsequent

TH1/2 cell expansion, and an anti-transgene humoral immune response to the virus and transgene.

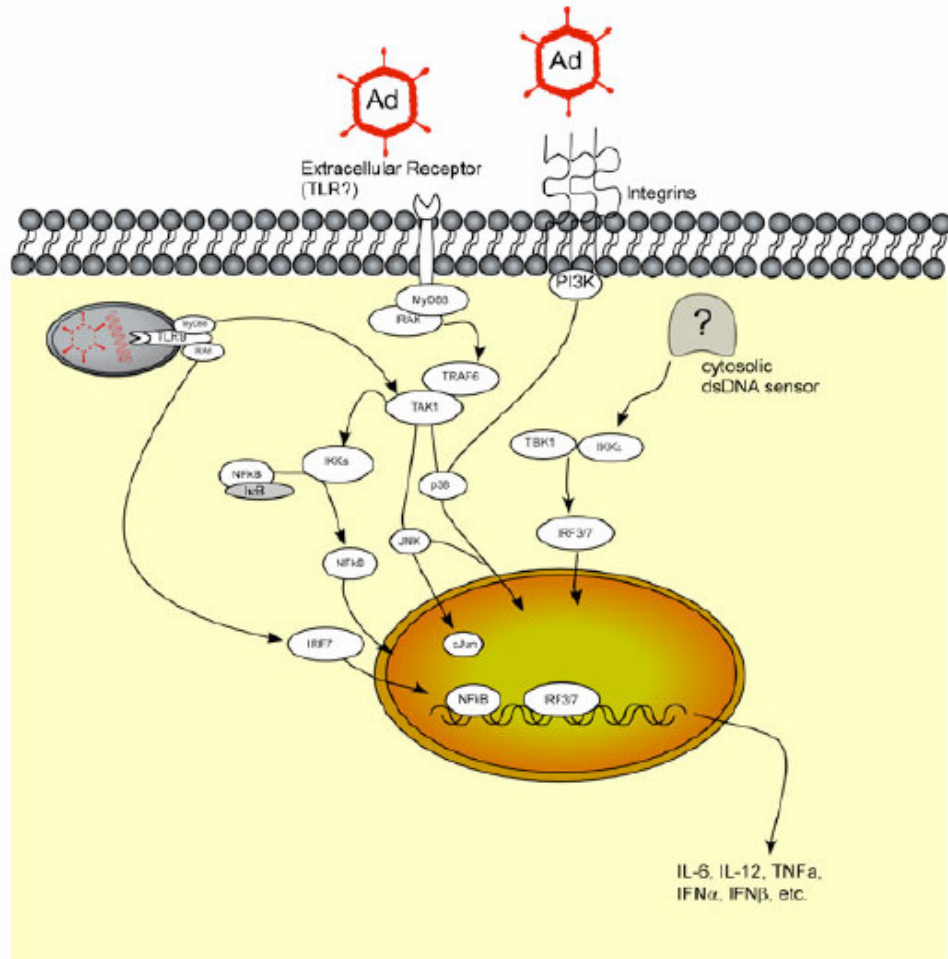


Figure 8. Molecular components of the innate cell-associated sensors of adenoviral infection.

Several components are responsible for the innate response to adenoviral vectors. The most important pathway involved in the production of cytokines are dependent by TLR and cytosolic sensors.

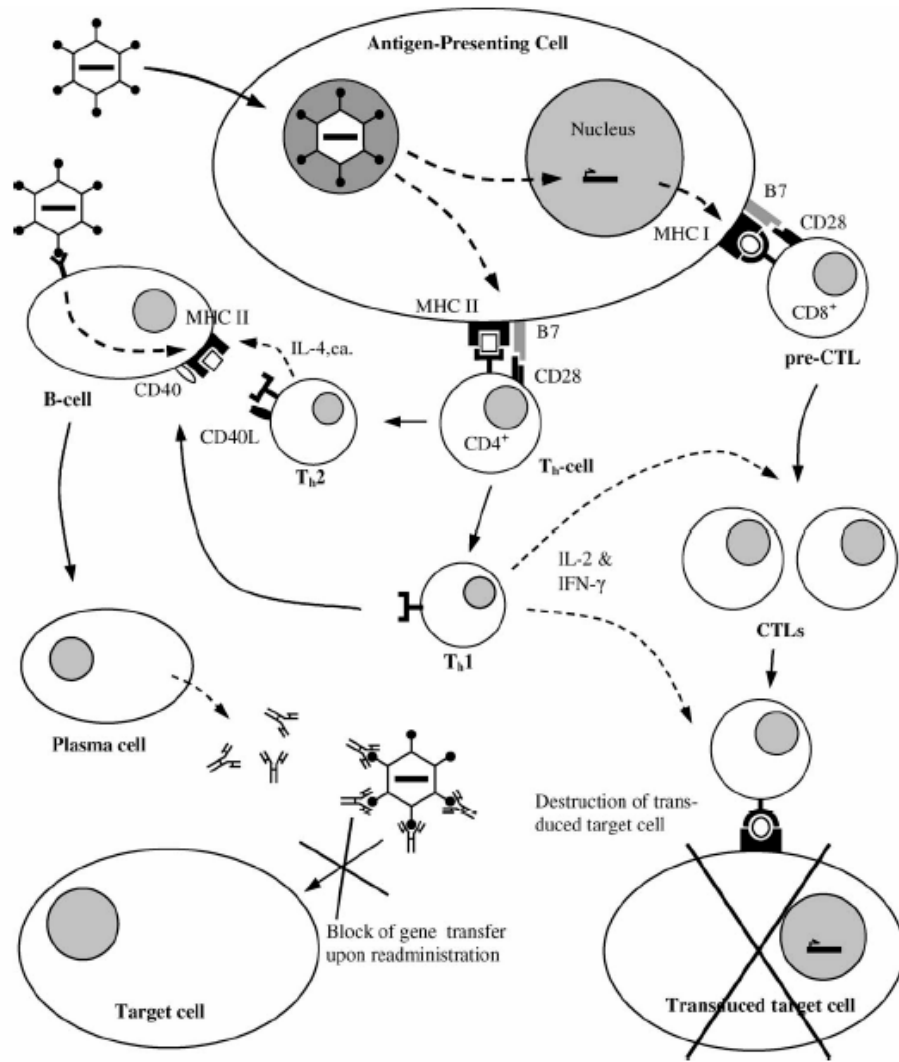


Figure 9. Activation of the host's immune system upon adenoviral gene transfer.

Antigen-presenting cells (APCs) process de novo synthesized viral proteins or transgene products and present these to CD8+ T cells by means of MHC class-I molecules. This causes the CD8+ T cells to form cytotoxic T lymphocytes (CTL), which specifically destroy the transduced target cells. The proliferation of CTLs is further stimulated by CD4+ helper cells of the Th1 subset. Their activation is triggered by epitopes from the input virus, which are presented by MHC class-II molecules on the cell surface of APCs. Apart from the cellular immune response, CD4+ T helper cells also participate in the activation of the humoral immune response. Binding of the Ad vector to B cells and interaction with an activated T helper cell induce B cells to differentiate into plasma cells. The subsequent production of Ad-specific neutralizing antibodies limits the beneficial effect of a repetitive administration of the same Ad vector by blocking its cellular entry.

this reason, chemical modification of viral capsid proteins, with the use of polyethylene glycol (PEG) (PEGylation), has been recently proposed as an alternative way to effectively ablate immune responses to adenoviral vectors. PEG is an uncharged, hydrophilic, non immunogenic polymer, with low toxicity. Moreover, it is approved by the Food and Drug administration (FDA) for use in drugs, foods and cosmetics. Currently, five PEG modified proteins are used in clinic: PEG-L-asparaginase, PEG-superoxide dismutase, PEG-adenosine deaminase, PEG-interleukin 2 and PEG- α -interferon, and in most cases, these proteins have shown improved therapeutic efficiency with enhanced circulation half life *in vivo*, reduced immunogenicity, enhanced solubility and suitable *in vivo* bioactivity. Indeed, PEGylation provides a hydrophilic coat to therapeutic molecules to protect them from proteolytic degradation and immune response, permitting an increase in the persistence of these proteins in the blood. The PEG can react also with the ϵ -amino terminal of lysine residues on the adenoviral capsid proteins, leading to a stable, secondary amine linkage. Different types of PEGs, differing in their molecular weight, can be used in this approach, but everyone binds the major structural Ads proteins (hexon, penton, base and fiber), that are the only proteins modified (O’Riordan, 1999). For this reason, factors, such as concentration of activated PEG, length of time of PEGylation and pH, can influence the retention of infectivity of PEGylated vectors. Indeed, a large number of PEG chains can couple to lysine residues in fiber knob and/or penton base and eventually may compromise the ability of the virion to interact with receptors on the cell surface. The modification of only 70% of available lysines results in a vector that efficiently evades the immune response, maintains the highest titer and its transduction efficiency (Croyle, 2000). Several studies on PEGylated Ad vectors have demonstrated a reduction in both innate and adaptive response in mice, both with the use of FG-Ad and HD-Ad vectors (O’Riordan, 1999; Croyle 2002; Croyle 2005): 1) 6 hours after systemical injection of the PEGylated vectors, the levels of serum cytokines were reduced, compared to treatment carried out with unmodified vectors; 2) 3 days after administration of PEGylated vector, no signs of thrombocytopenia were observed; 3) PEGylation of vectors also diminished the activation of cytotoxic T lymphocytes, helper T cells and the

production of neutralizing antibodies. These effects are due to a lesser recognition of the vector by macrophages, involved in the initial activation of both innate and adaptive immune response, but it is unknown the specific mechanism of PEG action and, in particular, the receptor/s on cell surface that is/are involved in the interaction with PEG. However, the PEGylation vectors show the same transduction efficiency of the unmodified vectors, associated with the possibility to readminister the native virus. All these advantages of PEGylated vectors render supposable their use in clinical trials.

4 Atherosclerosis.

4.1 Lipoprotein metabolism.

Lipoproteins are spherical particles present in blood plasma, containing a central core of non-polar lipids (triglycerides and cholesteryl esters) and a monolayer surface of polar lipids (phospholipids) and apoproteins. Reflecting the relative amounts of different lipids and proteins, the density of these particles is inversely related to their size and, so, it is possible to separate them in six main classes. The two largest classes, which contain mainly triglycerides in their core, are chylomicrons and VLDL (very low density lipoproteins). Instead, the smallest lipoprotein classes, LDL (low density lipoproteins) and HDL (high density lipoproteins) contain cholesteryl esters in their cores, while IDL (intermediate density lipoproteins) have an appreciable amount of both triglycerides and cholesterol.

Chylomicrons are synthesized and assembled in the endoplasmic reticulum of enterocytes, beginning from dietary fatty acids, as triglycerides (*Fig. 10*). Then, they are transported to the Golgi apparatus, where the nascent lipoproteins are packaged in secretory vesicles and delivered into the extracellular space by exocytosis. The beginning protein components include the apolipoprotein B-48 (ApoB-48) and ApoA-I, A-II and A-IV, but after the secretion they acquire ApoC-II and ApoE by transfer from HDL. Into the blood, chylomicrons bind to lipoprotein lipase, expressed on the surface of capillary endothelial cells that, in

presence of ApoC-II, mediates the hydrolysis of triglycerides. Concomitantly, some phospholipids, ApoC and ApoA are transferred to HDL: the residual particles are called chylomicrons remnant. The recognition of a domain on ApoE allows the binding of the remnants to LDL receptors on hepatocytes and so their endocytosis and catabolism in lysosomes. The cholesterol released from lysosomes in hepatocytes can enter in pathways leading to formation of bile acids. VLDL provide a pathway for export from hepatocytes of excess triglycerides and they are synthesized in the liver as a particles containing also ApoB-100 and small amounts of ApoE and C (*Fig. 10*). After secretion, additional amounts of the latter proteins are added and VLDL triglycerides are hydrolyzed in extrahepatic tissues by lipoprotein lipase to yield remnant particles. LDL receptors on hepatocytes recognize ApoE on VLDL remnants and mediate the endocytosis of a substantial fraction of these particles. Some particles, however, are further processed to IDL and then LDL that can be taken up by the same liver receptors (which recognize ApoB-100) or by LDL receptors on extrahepatic cells, even if the liver is the principal site of removal of LDL from the blood.

The plasma HDL are assembled extracellularly as surface components of triglyceride-rich lipoproteins, including phospholipids and cholesterol (*Fig. 10*). These components are transferred to pre-existing HDL particles from extrahepatic cells, and the cholesterol can be esterified by LCAT (lecithin-cholesterol acyltransferase) in presence of its main cofactor ApoA-I. The cholesteryl esters produced are rapidly transferred to other lipoproteins to be taken up into liver via the receptors mediated endocytosis. Therefore, the HDLs can be considered as the main particles involved in the reverse cholesterol transport, the process that mediates the transfer of cholesterol from extrahepatic tissue to the liver.

4.2 Plaque progression in atherosclerosis.

Atherosclerosis is an inflammatory process characterized by the deposition of lipid and other blood borne material within the arterial wall, that lead to the development of complex lesions, or plaques, protruding into the arterial lumen. Plaque rupture and thrombosis result in the acute clinical complications of

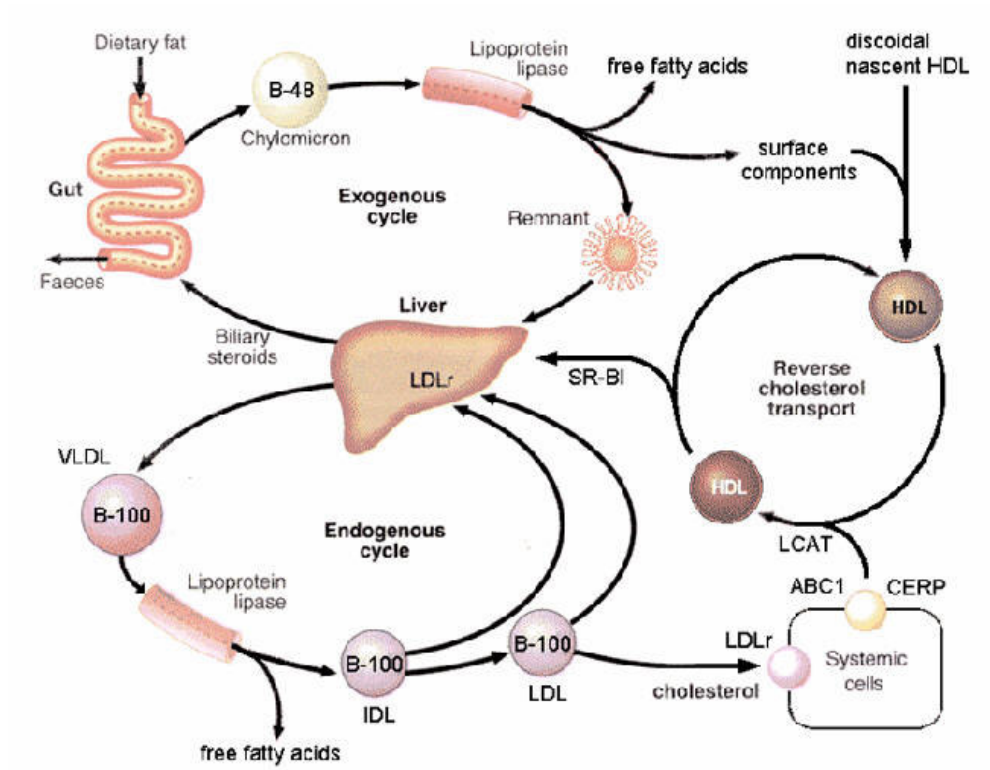


Figure 10. Schematic view of cholesterol metabolism and reverse cholesterol transport.

myocardial infarction and stroke. Among the several genetic and environmental risk factors, elevated level of serum cholesterol is probably the unique feature being sufficient to drive the development of atherosclerosis in humans and experimental animals.

The atherosclerosis lesions begin as a fatty streaks underlying the endothelium of large arteries, in particular in areas characterized by low shear rate and/or flow disturbances (bifurcation and branching points). Endothelial dysfunction has a considerable importance at the beginning of this process, because this dysfunction is characterized by a functional disruption of the protective endothelium, unleashing not only the internalization of cholesterol, but also the recruitment of inflammatory cells into the vessel wall, initiating the atherosclerosis process (**Fig. II**). At vascular level, the endothelial dysfunction is characterized by the synthesis and exposure of adhesive proteins (VCAM, ICAM, P and E selectin), facilitating the homing and internalization of the circulating monocytes and lipids into the intimal layer. Cholesterol accumulation plays a central role in atherogenesis: LDL can undergo oxidative modifications in the lipids and Apo-B, that can range from minimal modification (mmLDL) in which the LDL can still be recognized by LDL receptor, to extensive oxidations, that preclude the binding to the receptor. While LDL is protected from oxidation in the plasma compartment, it is thought that its retention by extracellular matrix proteins in the artery wall render it susceptible to enzymatic and nonenzymatic modifications. The presence of the oxidized lipids triggers a series of proinflammatory reactions via different mediators (TNF- α , IL-1, MCS-F), perpetuating the activation and recruitment of monocytes macrophages and inflammatory cells. Although the recruitment of monocytes to the arterial wall and their subsequent differentiation in macrophages may initially serve a protective function, by removing cytotoxic and proinflammatory oxidated LDL (oxLDL), progressive accumulation of these cells and their uptake to oxLDL ultimately leads to development of atherosclerotic lesions. In fact, macrophages, by accumulation of massive amounts of cholesterol esters, become foam cells. The uptake of cholesterol in these cells is mediated by scavenger receptors, that recognize oxidized phospholipids both in lipid phase and Apo-B. The macrophages have two potential mechanisms for depositing the

excess of cholesterol: enzymatic modification by cholesterol 27 hydroxylase, for converting it into a more soluble form, or the efflux via membrane transporters. The latter is the major mechanism with the HDL being the primary extracellular acceptor of cholesterol: this explains why risk of atherosclerosis is inversely correlated with the levels of HDL cholesterol. Once cholesterol has been taken up from HDL, it enters in the reverse transport of cholesterol and, so, it can be esterified by LCAT. At this point, HDL can exchange cholesterol esters for triglycerides carried by other lipoproteins via cholesterol ester transfer protein (CETP). Although the HDLs are the principal actors in reverse transport of cholesterol, ApoA-I is the real responsible for metabolic fate of HDL cholesterol, accounting for 70% of HDL protein content. Therefore, the overexpression of ApoA-I has a protective role in atherosclerotic progression.

The transition from a fatty streak to a more complex lesion is characterized by the immigration of smooth muscle cells from the medial layer of the artery wall to the intimal space (*Fig. 12*). Here, the smooth muscle cells may proliferate and take up modified lipoproteins, contributing to foam cells formation. Moreover, they synthesize extracellular matrix proteins that lead to the development of the fibrous cap. This phase of lesion development is influenced by the interaction between monocytes and activated T cells. The consequent cellular and humoral responses result in a chronic inflammatory state that, in association with the oxidized sterols present in oxLDL, appears to promote apoptosis and necrosis processes. Apoptosis of macrophages and vascular smooth muscle cells results from cell-cell interactions and the local cytokine environment within the arterial wall, involving the actions of pro and anti apoptotic proteins which include death receptors, proto oncogenes and tumor suppressor genes (*Fig. 13*). The necrotic cells release oxidated and insoluble lipids and matrix metalloproteases, that may influence the plaque stability and its rupture. Plaque rupture exposes plaque lipids and tissue factor to blood components, initiating the coagulation cascade, plaque adherence and thrombosis. These events are associated with acute myocardial infarction.

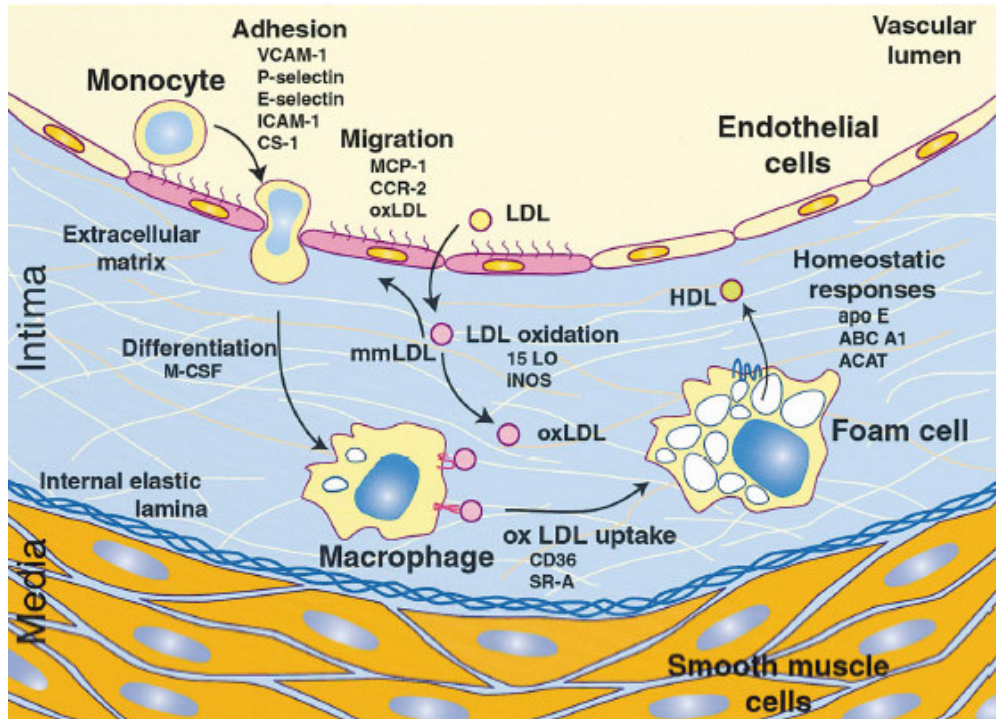


Figure 11. Initiating events in the development of a fatty streak lesion.

LDL is subject to oxidative modifications in the subendothelial space, progressing from minimally modified LDL (mmLDL), to extensively oxidized LDL (oxLDL). Monocytes attach to endothelial cells that have been induced to express cell adhesion molecules by mmLDL and inflammatory cytokines. Adherent monocytes migrate into the subendothelial space and differentiate into macrophages. Uptake of oxLDL via scavenger receptors leads to foam cell formation. OxLDL cholesterol taken up by scavenger receptors is subject to esterification and storage in lipid droplets, is converted to more soluble forms, or is exported to extracellular HDL acceptors via cholesterol transporters, such as *ABC-A1*.

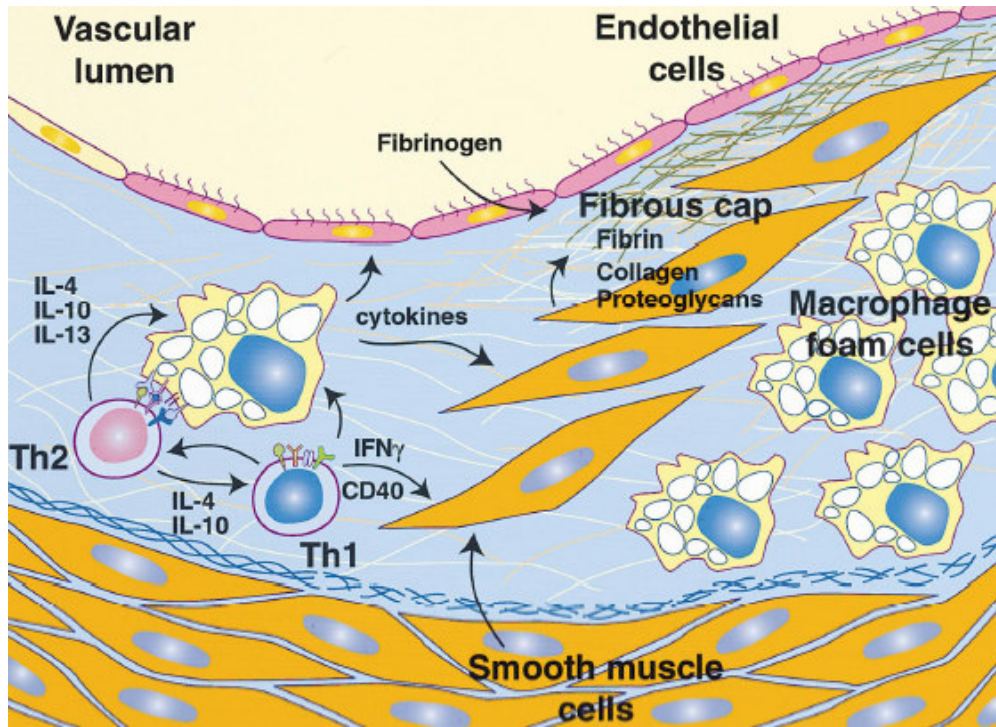


Figure 12. Lesion progression.

Interactions between macrophage foam cells, Th1 and Th2 cells establish a chronic inflammatory process. Cytokines secreted by lymphocytes and macrophages exert both pro- and antiatherogenic effects on each of the cellular elements of the vessel wall. Smooth muscle cells migrate from the medial portion of the arterial wall, proliferate and secrete extracellular matrix proteins that form a fibrous plaque.

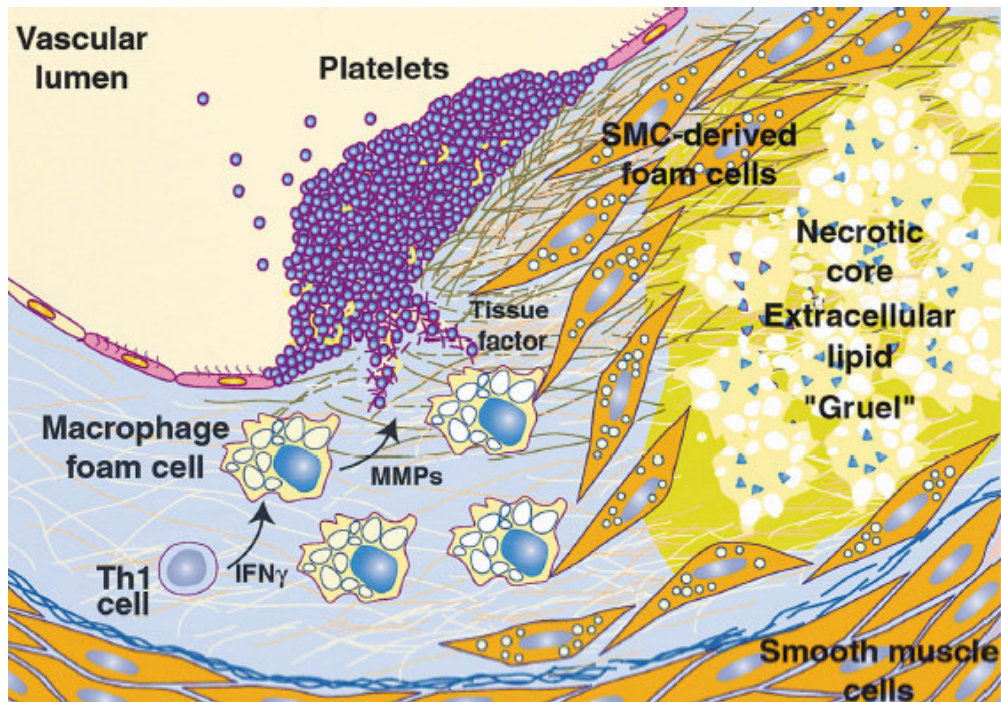


Figure 13. Plaque rupture and thrombosis.

Necrosis of macrophage and smooth muscle cell-derived foam cells leads to the formation of a necrotic core and accumulation of extracellular cholesterol. Macrophage secretion of matrix metalloproteinases and neovascularization contribute to weakening of the fibrous plaque. Plaque rupture exposes blood components to tissue factor, initiating coagulation, the recruitment of platelets, and the formation of a thrombus.

4.3 Animal models for atherosclerosis and preliminary data.

The ideal animal model of atherosclerosis should mimic the human subject, metabolically and pathophysiologically, and also develop lesions comparable to those found in humans. However, atherosclerosis is a complex multifactorial process, so no specie would ever be suitable for all studies. Mouse, for example, is an animal model largely used in the research but its differences with humans render complicate the translation of experimental results obtained with it. For example, the different lipid metabolism and gene expression make the wild type mice very resistant to the development of atherosclerosis. In fact in the mouse model, unlike humans, the primary circulating lipoprotein is the antiatherosclerosis HDL and the levels of LDL and VLDL are very low. Moreover, murine features like the location of atherosclerotic plaques (aorta in mice versus coronary arteries in humans), the course of the disease (fulminate in mice versus indolent in humans), the absence of end-stage ischemic lesions, as well as the fact that murine atherosclerosis is not associated with occlusive coronary artery disease, myocardial infraction, cardiac dysfunction, and premature death, which are the hallmarks of human coronary heart disease, might hinder the translation of the findings from mice to humans. Although mice are normally resistant to develop atherosclerosis, all of the current mouse models are based on perturbation of lipoprotein metabolism through both genetic manipulations and dietary. The most used mouse models are apolipoprotein E deficient mice (ApoE^{-/-}) and LDL receptor deficient mice (LDLR^{-/-}). The ApoE^{-/-} mice show a pronounced increase in the plasma levels of atherogenic lipoproteins, due to the failure of LDL receptor to mediate clearance of these lipoproteins. Moreover, even on a standard chow diet, which is low in its fat content, these mice have a spontaneous development of atherosclerotic lesions that can be strongly accelerated by a high fat diet. Nevertheless, the ApoE^{-/-} mouse model has a considerable limitation because plasma cholesterol is confined to VLDL and not to LDL particles as in humans. However, these mice are used in gene therapy as a model of familial hypercholesterolemia. Pastore et al. injected these mice, maintained on high fat diet, intravenously with a HD-Ad vector expressing the

entire human ApoA-I gene (Pastore, 2004). As a result of such a treatment, they showed supraphysiological levels of expression of transgene and a reduction of lesion size. In sum, using ApoA-I transgene, these mice showed a reduction of the development of atherosclerosis in absence of a significant liver toxicity.

The other animal model used in atherosclerosis studies is a mouse lacking the gene for LDLR ($LDLR^{-/-}$) whose mutations, in humans, cause familial hypercholesterolemia. The $LDLR^{-/-}$ mice display a modestly elevated plasma cholesterol level, when maintained on a regular chow diet, and develop only a slow atherosclerosis. When these mice are fed on high fat diet, they show a strong increase in plasmatic levels of cholesterol as well as a rapid development of atherosclerotic lesion. Interestingly, the plasma lipoprotein profile resembles that of humans, with the cholesterol being confined mainly to the LDL fraction. Also this animal model was used in gene therapy. The systemical injection of a vector expressing the entire gene of human ApoA-I, in mice maintained on a high-cholesterol diet for several weeks, leads to a small increase of plasma human ApoA-I, compared with control mice. Moreover, it is also possible to observe a delay in the atherosclerosis progression and a remodelling of the lesions to a more stable phenotype (Tangirala, 1999; Belalcazar, 2003). Obviously, the use of an HD-Ad vector permits a reduction in liver toxicity and a long-term hepatic ApoA-I expression (until 24 weeks), that cannot be pointed out in the same animals treated with a FG-Ad vector. The $LDLR^{-/-}$ mice, fed with a diet containing cholesterol and coconut oil, were also treated with murine VLDLR. Even in these experiments, after a single intravenous injection, plasma total cholesterol shows a reduction. In particular, the lowering is most marked in the fraction IDL/LDL, suggesting that the treatment leads to a marked reduction in the atherogenic potential of plasma lipoproteins. Moreover, the aortic atherosclerosis is prevented in these animals (Kobayashi, 1996; Oka, 2001). Recently, $LDLR^{-/-}$ mice fed with high cholesterol diet were treated systemically with a HD-Ad vector expressing the monkey LDLR (Nomura, 2004). This treatment resulted more effective than that performed by using HD-Ad-VLDLR both in lowering plasma cholesterol and in the progression of aortic atherosclerosis lesions. This is possible because LDLR binds, with high affinity, both ApoE and ApoB-100 containing lipoproteins,

whereas VLDLR binds with lower affinity solely ApoE containing lipoproteins. This difference underlies the fact that VLDLR mediates the uptake of only IDL but not LDL, whereas LDLR mediates the uptake of both IDL and LDL. However, some animals display anti-LDLR antibodies, with an obviously premature return of hypercholesterolemia. These observations suggest that the immune response to the vector and transgene product plays an important role in curtailing the therapeutic response to the treatment.

MATERIALS AND METHODS

1 Production of Helper-dependent adenoviral vectors.

Two HD-Ad vectors were used in the following studies. The first vector, HD-Ad-LacZ, contains the expression cassette for β -galactosidase gene under the control of the MCMV promoter (Palmer, 2003), while the second vector, HD-Ad-ApoA-I, contains 10 kb of the human APOA-I gene, including the promoter region (Belalcazar, 2003). Rescue and amplification of the vectors were performed using the HV-Ad-NG163R-2 helper virus as described. Briefly, 60-mm dish of 116 cells at 80% confluency were transfected with 20 μ g of *PmeI*-digested parental plasmid. Next day, the cells were infected with AdNG163R-2 at an m.o.i. of 1000 vp/cell. The vectors were amplified by serial coinfections of 60-mm dishes of 116 cells at 90% confluency with 10% of the crude lysate from the previous passage and HD-Ad-NG163R-2 at an m.o.i. of 200 vp/cell. After 3 infection in 60 mm dish, one 150-mm dish of 116 cells at 90% confluency was coinfecting with 10% of the crude serial passage 2 lysate and HD-Ad-NG163R-2 at an m.o.i. of 200 vp/cell. Large-scale HD-Ad production was performed in 3 liters of 116 cells ($3\text{--}4 \times 10^5$ cells/ml) coinfecting with 100% of the crude lysate from the 150-mm dish of serial passage 3 and HD-Ad-NG163R-2. 48 h later, coinfecting cells were harvested and HD-Ad virions were purified by two step of CsCl ultracentrifugations and dialyzed against 10 mM Tris-HCl pH 8.0, 4% (v/v) sucrose at 4 °C. Vector concentration was determined by UV spectrophotometric analysis at 260 nm. The title of HD-Ad-LacZ was also determined by X-gal staining on 293 cells as described previously (Ng, 2002) and expressed as BFU. Helper virus contamination was checked by Southern blot analysis on DNA extracted from the vector prep. Briefly, viral DNA was digested with *PstI* restriction enzyme and the hybridization was carried out at 55°C using HD-Ad-ITR probes; ECL plus was used as detection system. Helper virus was not detectable by Southern blot analysis and so the contamination can be considered <0,1%.

2 PEGylation of HD-Ad vectors.

The protein content of each viral preparation was determined with Bio-Rad DC Protein assay reagents and bovine serum albumin was used as standard. In total, 10 mg of monomethoxypoly(ethylene) glycol activated by succinimidyl succinate (SSPEG, mw 5000) was added for each microgram of protein present in each preparation. Conjugation reactions were performed at 25°C with gentle agitation. Reactions were stopped by addition of a 10-fold excess of L-lysine with respect to the amount of PEG added. Unreacted PEG, excess lysine, and reaction products were eliminated by buffer exchange over a second Econo-Pac 10DG disposable chromatography column, equilibrated with 100 mM potassium phosphate-buffered saline (pH 7.4). A separate aliquot of virus was treated and processed in the absence of SSPEG in the same manner as the conjugated virus and served as the unPEGylated control.

3 Characterization of PEGylated HD-Ad vectors.

PEGylated and unPEGylated adenoviral vectors were characterized by capillary zone electrophoresis using a Beckman PACE 5000 system with an untreated 50 $\mu\text{m}(\text{ID})\times 27$ cm capillary. The temperature of the capillary was controlled at 22°C. A preliminary 2 min wash in 1 N NaOH followed by a 2-min wash in nanopure water and a third wash in running buffer (20 mM sodium phosphate, pH 7.0, 5 mM sodium chloride) were performed prior to sample analysis. A voltage of 17 kV was used for the separations and the detector signal at 214 nm was recorded and processed by the PACE station software package.

4 Immunoturbidimetric assay.

The expression of human ApoA-I was evaluated by immunoturbidimetric analysis. 293 and W20-17 cells were infected with 200 vp/cell of HD-Ad-ApoA-I and PEG-HD-Ad-ApoA-I. Non infected 293 and W20-17 cells were used as

negative controls. Forty-eight hours after the infection, the medium was collected and a detergent solution was added at 37°C for 2 min. The absorbance at 610 nm was read (Abs1) and goat serum containing anti-human ApoA-I was added. The absorbance at 610 nm was read again (Abs2) and the concentration of human ApoA-I was calculated as $\Delta\text{Abs}=\text{Abs2}-\text{Abs1}$ on the calibration curve. Human serum with high and low concentration of ApoA-I was used as a positive control of the assay.

5 Animal studies.

MyD88^{-/-} mice were provided by S. Akira (Department of Host Defense, Research Institute for Microbial Diseases, Osaka University); TLR2^{-/-}, LDLR^{-/-} and C57BL/6 mice were purchased from Jackson laboratories. Food and water were provided *ad libitum*. All experimental procedures were conducted in accordance with institutional guidelines for animal care and use.

The mice used in the toxicity experiment were female 8-12 weeks old. Eight weeks LDL receptor-deficient (LDLR^{-/-}) female mice, on a C57BL/6 background, were fed on a diet supplemented with 0.2% (wt/wt) cholesterol and 10% coconut oil (vol/wt) for 4 weeks. HD-Ad was diluted in sterile PBS, prewarmed at 37°C, and injected into tail vein. The injections were performed in a total volume of 200 μl . Mice were anesthetized with Avertine before collecting blood from the retroorbital plexus. For cytokines analyses, blood was collected at 6 h and, for ALT determination, 3, 7 and 14 days postinjection. To analyse triglycerides, total cholesterol, LDL-C and HDL-C, blood was collected at 1, 2, 4, 8 and 12 weeks after vector administration from 12 hours fasting mice. Serum was frozen immediately and stored at -20°C until analyses. For β -galactosidase staining, mice were killed 48 h postinjection. Upon sacrifice, the liver was harvested and kept on dry ice or at -80°C until analyses. To analyse atherosclerotic lesion, mice were sacrificed 12 weeks after the treatment and aortas were taken.

6 Evaluation of toxicity.

Mouse IL-6 and MCP-1 was assayed by using the BD cytokine multiplex bead array system and analyzed using a BD FACSArray instrument, according to manufacturer's instructions. Briefly, beads against these cytokines were mixed to 10 µl of serum and incubated at room temperature for 1 hour. PE detection reagent was added and incubated again in the same conditions. Samples were run at FACSArray and the data were analysed by FACSArray System Software.

IL-12p40 was assayed by Immunoassay kit according to the manufacturer's instruction.

Mouse ALT levels were measured enzymatically on 100 µl of serum by using Vitros 250 Analyser, based on spectrophotometric dry chemistry.

7 X-Gal staining and β-Gal enzyme assay.

For X-gal staining, liver samples from each animal were embedded in Tissue-Tek O.C.T. compound and frozen until used for sectioning. Frozen sections (8 µm) were prepared on a refrigerated microtome and fixed with 1.25% glutaraldehyde at 4°C for 10 minutes. Slides were rinsed twice with PBS and immersed in X-gal (5-bromo-4-chloro-3-indolyl-β-D-galactosidase) solution.

For β-galactosidase determination, total proteins were extracted from the liver and the enzyme activity was determined using β-Galactosidase Enzyme Assay System with Reporter Lysis Buffer. Protein content was determined with the Micro BCA protein assay reagent kit using BSA as standard.

8 Lipids measurement.

Mouse triglycerides, total cholesterol, HDL-C and LDL-C levels were measured enzymatically on 100 µl of serum by using Vitros 250 Analyser, based on spectrophotometric dry chemistry.

9 Dissections of aortas and quantization of atherosclerotic lesions.

Twelve weeks after treatment, mice were sacrificed and aortas, from heart to iliac branching, were dissected out. Briefly, mice were euthanized and the viscera were cut out. Then, aortas were dissected out and fat and leftover tissues carefully cut out until aortas were clean, to proceed, thereafter, with their opening. To quantize the intimal fat, aortas were fixed in 4% Buffered Formal Saline solution and stained with Oil Red O. Images were acquired using Sigma Scan Pro and the fat amount were quantified with NIS elements program.

10 Statistical analysis.

Results were analysed using two-way (treatment-time) ANOVA with repeated measures, followed by Fischer's post-hoc comparison when required. A significance level of $p < 0,005$ was accepted as statistically significant. All measures are expressed as mean \pm standard error of the mean (S.E.M.). All statistical analyses were performed with StatView software (version 567 5.0.1.0; SAS Institute, Cary, NC).

RESULTS

1 Production and characterization of HD-Ad vectors.

The HD-Ad plasmid expressing LacZ, p Δ 28E4LacZ, was constructed at Baylor College of Medicine in Houston by Ng, as follows: the 3.6-kb *Psh*AI fragment was replacing from p Δ 28E4 with the Klenow-treated 4.7-kb *Xba*I–*Bgl*II fragment, containing the MCMV–LacZ expression cassette from pCA35. To a large scale production, the 29.3-kb HD-Ad, HD- Δ 28-E4-LacZ, was rescued following *Pme*I digestion of p Δ 28E4LacZ and transfected in 116Cre4 cells and 24 hours after the transfection, the cells were infected with the helper virus, AdNG163R-2, to permit the assembly of virions. Several passages of infections of adherent 116Cre4 cells with the lysates of 60mm dishes and AdNG163R-2 were carried out until the coinfection of 2 liters of 116Cre4 cells growing in suspension. Forty-eight hours post coinfection, we purified HD- Δ 28-E4-LacZ by ultracentrifugation in continuous CsCl gradient (**Fig. 14 A**). Spectrophotometric analysis revealed that we obtained a total yield of 1×10^{13} vp (viral particles) corresponding to about 25000 vp/cell. To analyze the ratio between the infection particles and the viral particles expressing LacZ, an X-gal staining was performed on 293 cells: the HD- Δ 28-E4-LacZ was 8×10^{11} BFU (blue forming units)/ml, for a ratio vp:BFU of about 10:1. To use this HD- Δ 28-E4-LacZ for *in vivo* toxicity studies, we had also determined the helper virus contamination through Southern blot analysis of viral DNA using the ITR probe hybridized to *Pst*I-digested DNA. As shown in figure 14 B (**Fig. 14 B**) the helper virus contamination was undetectable and this was consistent with a contamination of less than 0,1%. Indeed, HD- Δ 28-E4-LacZ had the same structure of the parental plasmid, p Δ 28E4LacZ (line 1 and 3 of figure 14 B). At University of Texas in Austin, a part of the vector HD Δ 28E4LacZ had undergone the PEGylation reaction, that, based upon previous experience with PEGylation of viral vectors (Croyle, 2005), was carried out for 2 hours at room temperature. Changes in the surface properties of the viral capsid, due to the bind with PEG, was monitored by capillary electrophoresis (**Fig. 15**). Unmodified HD-Ad, which has treated according to PEGylation protocol but without adding PEG,

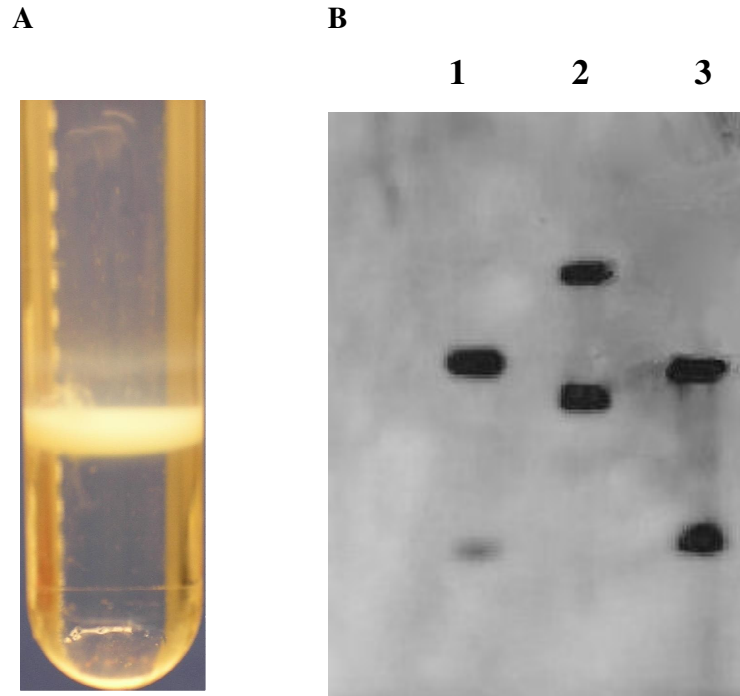


Figure 14. HD- Δ 28-E4-LacZ purification and helper virus contamination.

(A) HD-D28-E4-LacZ after ultracentrifugation in continuous CsCl gradient. (B) Southern blot analysis of plasmid and viral DNA to verify helper virus contamination. Plasmid and viral vector were digested with *Pst*I and fractionated on a 1% agarose gel. Southern blot analysis was performed using a probe hybridized on ITRs. Lane 1, HD-D28-E4-LacZ; lane 2, AdNG163R-2; lane 3, p Δ 28E4LacZ.

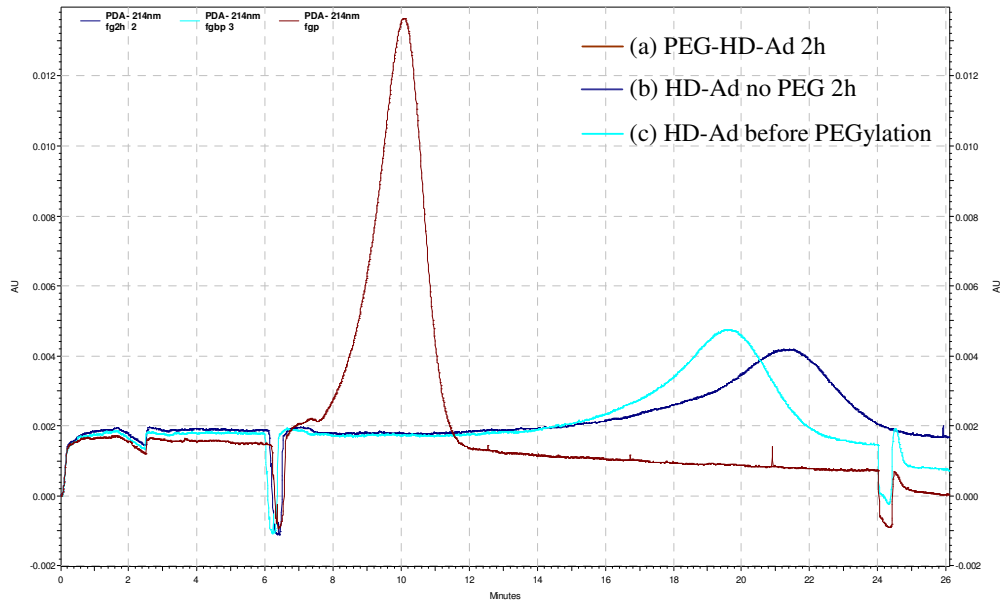


Figure 15. Capillary electropherogram.

Representative capillary electropherograms of (a) HD-D28-E4-LacZ (b) unmodified HD-D28-E4-LacZ (c) HD-D28-E4-LacZ after the ultracentrifugation, before PEGylation. Samples were diluted 1:2 with sample buffer (20 mM sodium phosphate buffer, pH 7.0, 5 mM sodium chloride). Capillary length was 27 cm. Virus was detected at 214 nm. AU, absorbance units.

had a peak at about 22 minutes. This peak was superimposable to that obtained with the HD-Ad collected after the CsCl ultracentrifugation. Indeed, the PEG-HD-Ad vector was detected as a single peak at 10 minutes and the unmodified vector was absent from PEGylated preparation, indicating that all viral particles had reacted with PEG.

The HD-Ad plasmid containing the entire human ApoA-I gene, p Δ 21ApoA-I, was obtained at Baylor College of Medicine in Houston by Belalcazar, as follows: 10 kb of the human ApoA-I gene, including the promoter region, was inserted into the pLPBL1 plasmid and subcloned into the unique *Asc*I site of the p Δ 21 plasmid, that contained the inverted terminal repeats, the packaging signals of adenovirus type 5 and DNA stuffer from the human HPRTB gene and the cosmid C346. The corresponding vector, HD-Ad-ApoA-I, was obtained according the protocol used for the HD- Δ 28-E4-LacZ. Also for HD-Ad-ApoA-I, the spectrophotometric analysis was made: the concentration of vector resulted been 7×10^{12} vp/ml. To assay helper virus and PEGylation reaction, the Southern blot and capillary electrophoresis were carried out but obviously the data are not show because the probe used in Southern blot hybridized on ITRs, which are the some for all vectors, and the peaks obtained from capillary electrophoresis are very similar to the previous. However, to evaluate the levels of expression of human ApoA-I, 293 and W20-17 cells (a mouse cell line) were infected with HD-Ad-ApoA-I modified and unmodified and the human ApoA-I secreted in the medium was measured with an immunoturbidimetric assay. As shown in figure 16 (**Fig. 16**) both 293 and W20-17 cells had very low basal levels of secreted ApoA-I ($17 \pm 3,5$ ng/ μ l and $13 \pm 0,3$ ng/ μ l, respectively). The infection with HD-Ad-ApoA-I or PEG-HD-Ad-ApoA-I led to an increase in the secretion of the protein of about 4 folds in 293 (77 ± 28 ng/ μ l) and 2 in W20-17 cells (27 ± 6 ng/ μ l), when they were infected with unmodified vector, or about 3 folds (54 ± 8 ng/ μ l) and 2,5 (32 ± 6 ng/ μ l) in 293 and W20-17 respectively. The lower secretion of ApoA-I in W20-17 cells than in 293 was probably due to a lesser infectivity of these cells. Indeed, there were no significant differences in the secretion of ApoA-I when the cells were treated with HD-Ad or PEG-HD-Ad vector. This data confirms the functionality

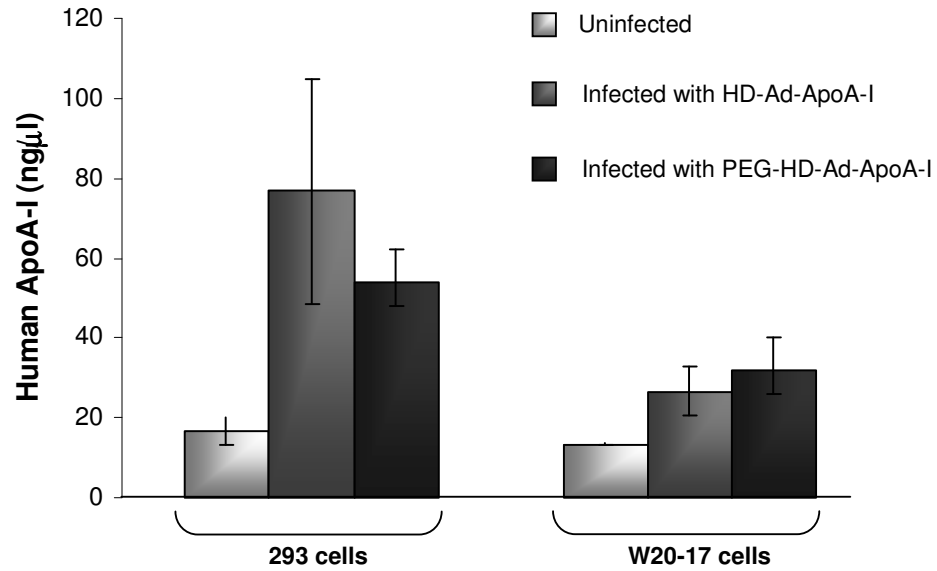


Figure 16. Immunoturbidimetric assay.

293 and W20-17 cells were infected with HD-Ad-ApoA-I and PEG-HD-Ad-ApoA-I and the secreted protein were measured. Non infected 293 and W20-17 cells were used as negative controls. The infection with the vectors led to an significant increase in the secretion of human ApoA-I in both cells lines compared with uninfected cells.

of both vectors and that the PEGylation reaction do not influence the expression of transgene. In short these vectors can be used for *in vivo* studies.

2 Role of MyD88 in the acute inflammatory response triggered by systemic HD-Ad administration.

To investigate the role of MyD88 in Ad acute toxicity, MyD88^{-/-} mice in C57BL/6 background (N=5) were injected with 1x10¹³ vp/kg of HD-Ad vector expressing LacZ driven by the ubiquitous CMV promoter (HD-Ad-LacZ). Blood samples were collected 6 hours after the injection for platelets, AST, ALT and cytokine (IL-6 and IL-12) determinations and the results from MyD88^{-/-} mice were compared to those generated in C57BL/6 (WT) controls (N=5) injected under the same identical conditions. No difference in the levels of both AST and ALT were observed between the two groups of mice (data not shown). Also, similar reduction in platelet counts was noted among the two mouse strains (data not shown). However, MyD88^{-/-} mice showed a drastic (more than 80%) reduction in IL-6, (1,200 pg/ml ± 200 in WT treated mice vs 200 pg/ml ± 59 in MyD88^{-/-} treated mice; p<0,002) (**Fig. 17 A**), and an approximately 60% of reduction in IL-12 (1065 pg/ml ± 80 in WT-treated mice vs 404 pg/ml ± 180 in MyD88^{-/-} treated mice; p<0,03) (**Fig. 17 B**). Although less prominent, reduction in MCP-1 levels was also observed (**Fig. 17 C**). In the same mice sampled for cytokine levels, liver samples collected on day 3 post-injection were assayed for β-galactosidase activity to determine transduction efficiency and no significant difference in transduction efficiency were noted between the MyD88^{-/-} and control mice (**Fig. 18**). Therefore, the reduction in cytokines levels is not accompanied to a reduction in efficiency liver gene transfer. These results show that MyD88 is a major player in the activation of the proinflammatory acute response following systemic Ad vector administration. Being a crucial component of the downstream activation pathway of several TLRs, and considering previous studies, showing that TLR9 has a relatively minor role in Ad acute toxicity, we hypothesized that other TLRs are likely to be involved through MyD88 activation in the acute inflammatory response triggered by Ad vectors.

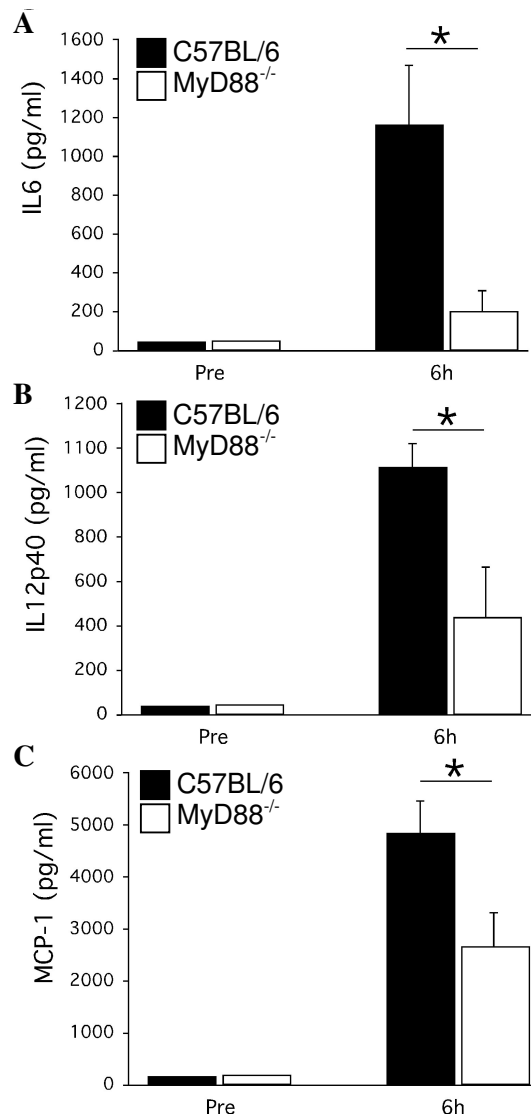


Figure 17. MyD88 role in the innate response to HD-Ad.

MyD88^{-/-} mice in C57BL/6 background were injected with 1×10^{13} vp/kg HD-Ad-LacZ. C57BL/6 mice were injected with the same dose as a control. Six hours after the injection plasma samples were collected and cytokines levels were assayed. **(A)** IL-6 was assayed by FACSARRAY. **(B)** IL-12p40 was assayed by ELISA. **(C)** MCP-1 was assayed by FACSARRAY as described in Material and Methods. * $p < 0,05$; ** $p < 0,03$

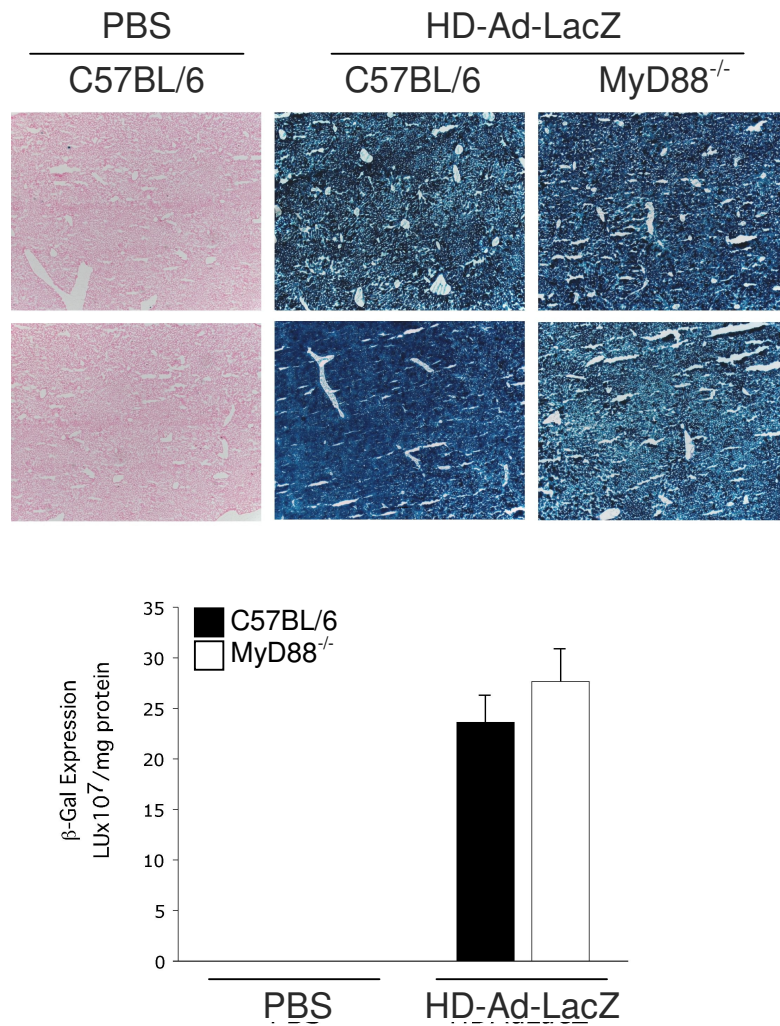


Figure 18. Hepatocyte transduction following systemic injection of HD-Ad-LacZ in C57BL/6 and MyD88^{-/-} mice.

MyD88^{-/-} and C57BL/6 mice were injected with 1×10^{13} vp/kg of HD-Ad-LacZ. C57BL/6 mice were injected with the same dose as control. 72 hours after vector administration, livers were collected for analysis. Another cohort of mice were injected with PBS as negative control. (A) X-Gal staining of liver from C57BL/6 and MyD88^{-/-} mice following administration of the vector. PBS was used as negative control. (B) β-galactosidase expression from liver from C57BL/6 and MyD88^{-/-} mice.

3 TLR2 deficiency attenuates the innate immune response to HD-Ad vectors *in vivo*.

Being a crucial component of the downstream activation pathway of several TLRs, and considering previous studies, showing that TLR9 has a relatively minor role in Ad acute toxicity, we hypothesized that other TLRs are likely to be involved through MyD88 activation in the acute inflammatory response triggered by Ad vectors.

TLR(s) expressed on the plasma membrane would be good candidates and therefore we decided to start investigating the role of TLR2 which is known to localize on the plasma membrane. To this end, we analyzed the cytokine activation profile in TLR2^{-/-} mice, in C57BL/6 background, administered with different doses of HD-Ad as compared to a control group (C57BL/6 mice) injected with the same vector at the same doses. TLR2^{-/-} mice (N=5 per treatment group) were injected with either 5x10¹² or 1x10¹³ vp/kg of HD-Ad-LacZ. TLR2^{-/-} mice were found to have a less severe increase of proinflammatory cytokines compared to the control group (**Fig. 19**). Blood samples for cytokine analyses were collected at 6 hours and liver samples for quantitative β-galactosidase activity at 72 hours post-injection. At the dose of 1x10¹³ vp/kg, the IL-6, IL-12 and MCP-1 levels were found to be significantly different between TLR2^{-/-} (600 ± 150 pg/ml, 452 ± 198 pg/ml and 1750 ± 328 pg/ml, respectively) and C57BL/6 mice (1350 ± 108 pg/ml, 998 ± 89 pg/ml and 3500 ± 553 pg/ml, respectively). Also at the lower dose of 5x10¹² vp/kg, IL-6, IL-12 and MCP-I were assayed, and consistently with previous data, IL-6 levels were significantly reduced in TLR2^{-/-} mice (270 ± 123 pg/ml) as compared with C57BL/6 mice (550 ± 118 pg/ml) (p<0.03). Similarly, IL-12 levels in TLR2^{-/-} mice were 260 ± 103 pg/ml while in C57BL/6 mice were 554 ± 102 pg/ml (p<0.05). The hepatocyte transduction was essentially the same among the treated groups (**Fig. 20**).

Taken together, these data show that TLR2 is an important early sensing receptor in the activation of the acute inflammatory response to HD-Ad vectors *in vivo*.

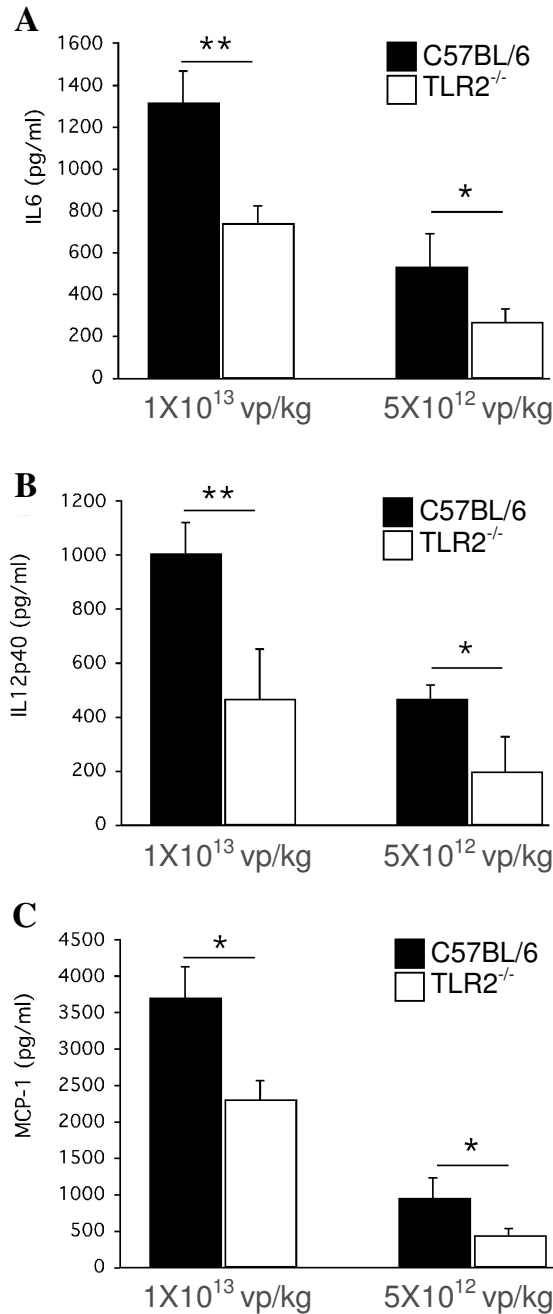


Figure 19. TLR2 deficiency attenuates innate immune response to HD-Ad *in vivo*.

Two groups of TLR2^{-/-} were injected with two different doses (5x10¹² vp/kg and 1x10¹³ vp/Kg) of HD-Ad-LacZ. C57BL/6 mice were injected with the same doses as control. Six hours after the injection plasma samples were collected and cytokine levels were assayed. IL-6 (A) and MCP-1 (C) levels were measured by FACSARRAY. IL-12 (B) levels were measured by ELISA.**, p<0,03; *, p<0,05

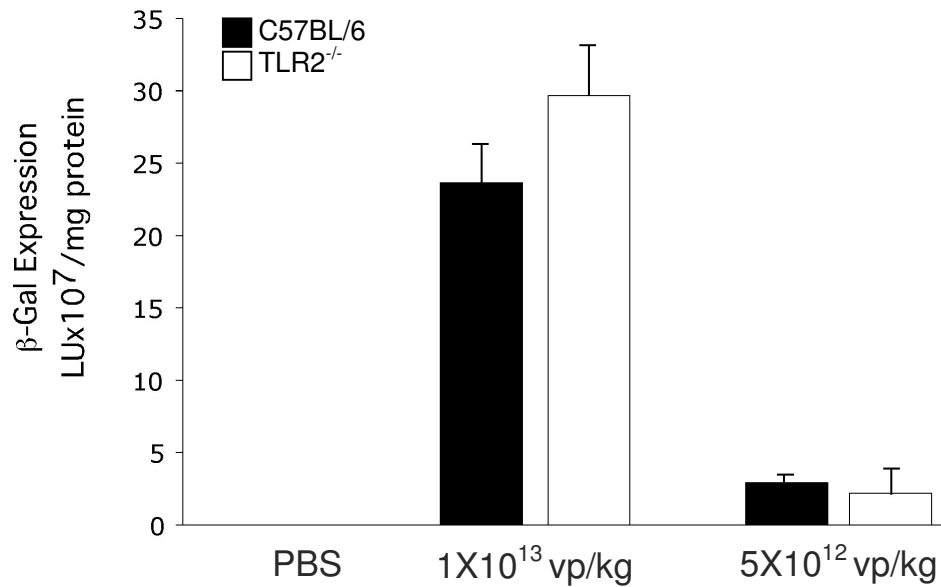


Figure 20. Hepatocyte transduction following systemic injection of HD-Ad-LacZ in C57BL/6 and TLR2^{-/-} mice.

TLR2^{-/-} mice were injected with either 5x10¹² and 1x10¹³ vp/kg of HD-Ad-LacZ. C57BL/6 mice were injected with the same doses as control. 72 hours after vector administration livers were collected and homogenized for β -galactosidase expression assay. Another cohort of mice were injected with PBS as negative control.

4 PEGylation masks the interaction between HD-Ad and the TLR2.

Several groups have demonstrated that systemic administration of PEGylated Ad into mice resulted in a 50% to 70% reduction in serum IL-6 compared to unPEGylated vector without compromising hepatic transduction efficiency. The mechanism responsible for this effect is unclear and we hypothesized that the PEG could mask the vector from TLRs activation. We have therefore investigated the activation of the proinflammatory cytokines (IL-6, IL-12) in MyD88, TLR9 and TLR2 knock-outs, and C57BL/6 control mice at 6 hours after the injection of 1×10^{13} vp/kg of either PEGylated or unPEGylated HD-Ad-LacZ. As previously reported, there were significant cytokine reductions of 40-45% between PEGylated and unPEG HD-Ad in C57BL/6 mice. Indeed, IL-6 value was 550 ± 78 pg/ml in the group of mice injected with HD-Ad-LacZ while it was 250 ± 123 pg/ml in mice treated with PEG-HD-Ad-LacZ ($p < 0.05$) (**Fig. 21 A**). Also IL-12 value was different among the group of mice injected with HD-Ad-LacZ and that treated with PEG-HD-Ad-LacZ (554 ± 102 pg/ml vs 226 ± 156 pg/ml, respectively; $p < 0.05$) (**Fig. 21 B**). However, no significant differences in both IL-6 and IL-12 were noted between MyD88^{-/-}, TLR9^{-/-} and TLR2^{-/-} mice (**Fig. 21 A, B**). Indeed, in MyD88^{-/-} mice, IL-6 value was 148 ± 39 pg/ml in mice injected with HD-Ad-LacZ versus 159 ± 43 pg/ml in PEG-HD-Ad-LacZ receiving group (**Fig. 21 A**), instead IL-12 value was 128 ± 42 pg/ml in the animal treated with HD-Ad-LacZ versus 96 ± 40 pg/ml in the group of mice injected with PEG-HD-Ad-LacZ (**Fig. 21 B**). The same difference, in IL-6 and IL-12 levels, were showed in TLR9 KO mice: IL-6 value was 387 ± 59 pg/ml vs 298 ± 83 pg/ml and IL-12 value was 322 ± 68 pg/ml vs 284 ± 21 pg/ml, respectively in mice administrated with HD-Ad-LacZ and PEG-HD-Ad-LacZ vectors (**Fig. 21 B**).

Being the TLR9 expressed in the endosome and activated by esogenous DNA, it is not expected to be affected by vector PEGylation. The IL-6 levels, in TLR2^{-/-} mice, were comparable between mice injected with HD-Ad-LacZ and PEG-HD-Ad-LacZ (**Fig. 21 A**). Also IL-12 values were not significantly different between

HD-Ad-LacZ and PEG-HD-Ad-LacZ treated mice (*Fig. 21 B*). The β -galactosidase assay on liver samples showed no significant differences in hepatocytes transduction efficiency (data not shown).

Taken together these data show the lack of protective effect of PEG on the activation of the pro-inflammatory cytokines in MyD88^{-/-} and TLR2^{-/-} mice consistently with the hypothesis that PEG prevents adenoviral vector from activation of TLRs. The residual cytokine response observed suggests that other pathways independent from the TLR are activated by systemic Ad administration.

5 Toxicity of HD-Ad-ApoA-I and PEG-HD-Ad-ApoA-I in a mouse model of atherosclerosis.

As above mentioned, we have shown that PEG molecules can hide the viral capsid proteins to the immune system cells. In particular, the ability of PEG to mask the interaction of vector with TLR2 leads to a mitigating proinflammatory cytokine activation. This important observation needs to be corroborate in a model of pathology, to eventually proceed with clinical studies. To this aim, we tested PEGylated and non PEGylated HD-Ad vector expressing ApoA-I in a mouse model of atherosclerosis. Eight weeks old LDLR^{-/-} mice (N=5) were fed on high cholesterol diet for 4 weeks and then injected systemically with 1×10^{13} vp/kg of HD-Ad-ApoA-I or PEG-HD-Ad-ApoA-I. Control animals (N=5) were treated with an equal volume of PBS. At different time points (0, 6, 24 and 72 hours), blood samples were collected to analyse the serum levels of IL-6, the main marker of inflammation. At 0 hours, as expected, there were no differences among groups, but after the administration of the vectors, an increase in proinflammatory cytokine was observed (*Fig. 22*). In particular, mice treated with HD-Ad-ApoA-I showed a strong increase of serum levels of IL-6 compared to animals receiving PEG-HD-Ad-ApoA-I (1300 ± 300 pg/ml and 400 ± 61 pg/ml, respectively; $p = 0,001$) (*Fig. 22 A*). However, in both treated animals groups, IL-6 levels returned at basal levels starting from 24 hours.

Within the same groups of animals, we measured alanine transaminase (ALT), as index of liver vectors-induced toxicity. Blood samples were collected for ALT

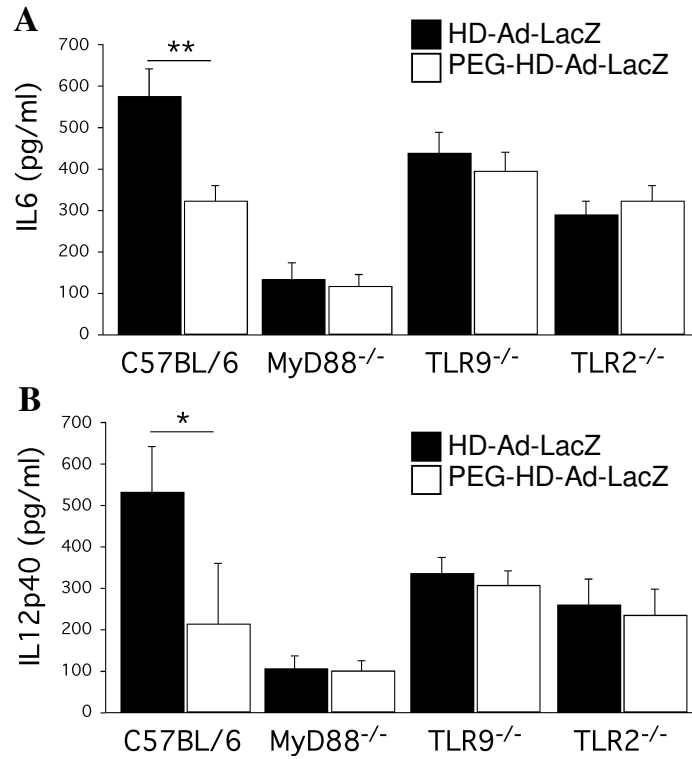


Figure 21. PEG protects viral vector from interaction with TLRs family.

MyD88^{-/-}, TLR9^{-/-} and TLR2^{-/-} were injected with 1×10^{13} vp/kg, C57BL/6 mice were used as controls. Blood samples were collected 6 hours after vector administration and cytokines analysis was performed. **(A)** IL-6 was assayed by FACSARRAY. **(B)** IL-12p40 was assayed by ELISA. **, $p < 0,03$, *, $p < 0,05$.

determination at 0, 3, 7, 14 days after the injection: as for IL-6, at 0 day, there were no differences among the groups (**Fig. 22 B**). Differently to proinflammatory cytokines, at different time points (3, 7 and 14 days), ALT values did not undergo changes from baseline, in animals treated with both PEGylated and non PEGylated vector. As shown in previous works (Croyle, 2005), this data confirms that HD-Ad-vectors have a very low liver toxicity, which is independent from capsid modification.

6 HD-Ad-ApoA-I, but no PEG-HD-Ad-ApoA-I, induces effects in blood lipidic pattern.

To evaluate the effects of overexpression of human ApoA-I on the cholesterol metabolism, 8 weeks old LDLR^{-/-} mice (N=5), maintained on an atherogenic diet for 4 weeks, were injected into tail vein with 1×10^{13} vp/kg of HD-Ad-ApoA-I or PEG-HD-Ad-ApoA-I. Another group of animals (N=5) was used as negative control and received, systemically, an equal volume of PBS. Triglycerides, total cholesterol, LDL-cholesterol (LDL-C) and HDL-cholesterol (HDL-C) were measured at different weeks (1, 2, 4, 8 and 12 weeks) after the administration of the vectors. Basal plasma triglycerides were 97 ± 5 mg/dL in control mice, $88,5 \pm 3$ mg/dL in HD-Ad-ApoA-I treated mice and $97,3 \pm 2$ mg/dL in mice receiving PEG-HD-Ad-ApoA-I (**Fig. 23 A**). These levels were not modified by the expression of human ApoA-I. Indeed, during weeks, there were no differences among groups, treated and not, compared with triglycerides value at 0 time.

About total cholesterol, its basal levels were 520 ± 60 mg/dL, 536 ± 50 mg/dL, 550 ± 100 mg/dL in PBS, HD-AD-ApoA-I and PEG-HD-Ad-ApoA-I injected mice, respectively (**Fig. 23 B**). After a single administration of HD-Ad-ApoA-I, an increase in total cholesterol was observed. This value reached a peak at 4 weeks, showing a considerable difference from control mice (730 ± 30 mg/dL vs 450 ± 80 mg/dL; $p = 0,006$). Total cholesterol levels persisted at high values until the end of the experiment at 12 weeks. Instead, the administration of PEG-HD-Ad-ApoA-I did not induce any effects on the total cholesterol levels, which

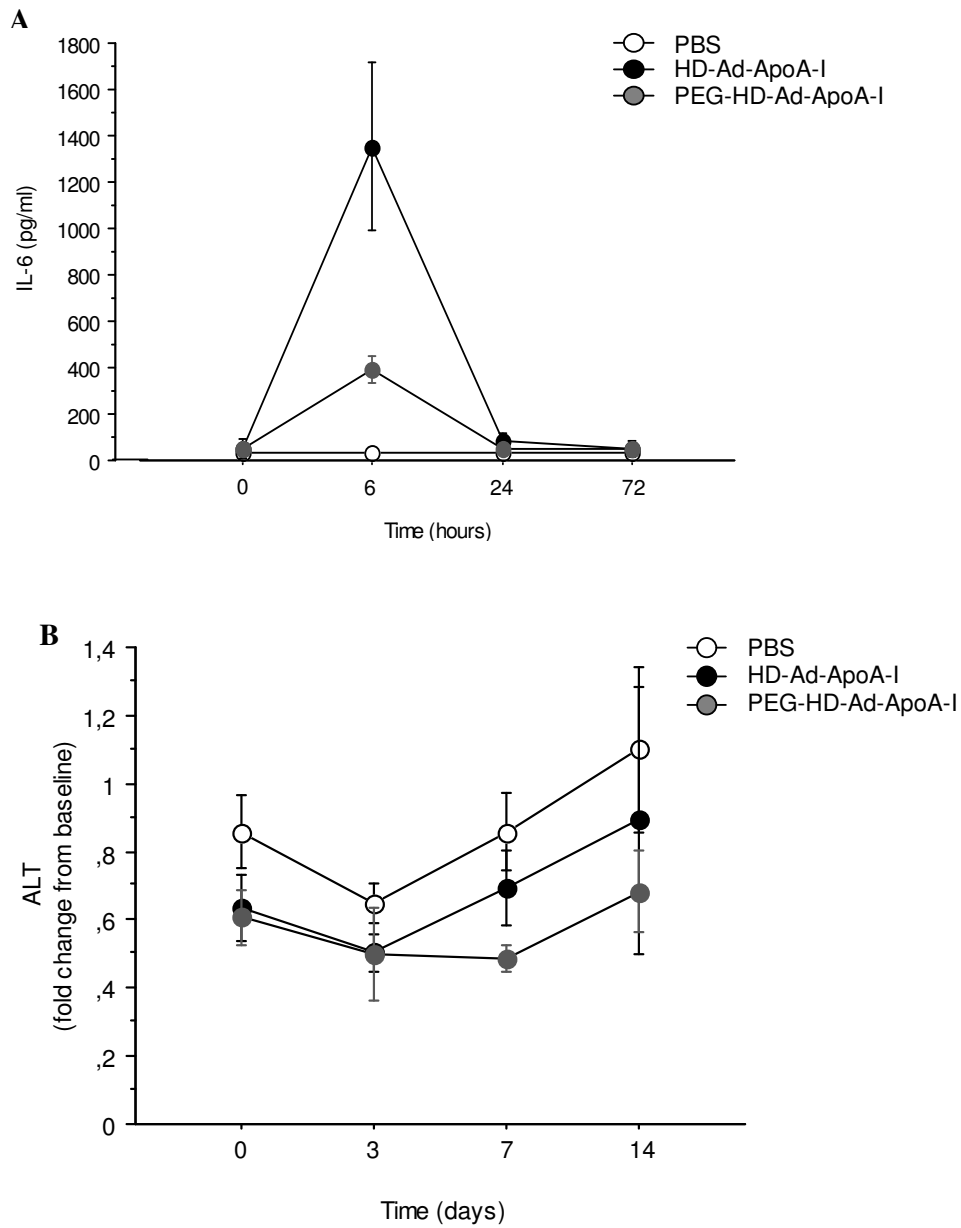


Figure 22. HD-Ad-ApoA-I and PEG-HD-Ad-ApoA-I toxicity.

LDLR^{-/-} mice were injected systemically with 1×10^{13} vp/kg of HD-Ad-ApoA-I and PEG-HD-Ad-ApoA-I. Mice treated with a same volume of PBS were used as control. At 6, 24 and 72 hours after the injection, blood samples were collected. IL-6 levels (**A**) were analysed by FACSARRAY. At 3, 7 and 14 days after treatment, ALT levels (**B**) were assayed on blood samples.

remained at values comparable to baseline also at 4 weeks (350 ± 77 mg/dL), when cholesterol in HD-Ad-ApoA-I injected mice reached the highest levels.

To evaluate the influence of ApoA-I on reverse transport of cholesterol, we also analysed serum levels of LDL-C and HDL-C. The basal LDL-C level was comparable among the 3 groups (389 ± 55 mg/dL, 399 ± 57 mg/dL and 420 ± 100 mg/dL in PBS, HD-Ad-ApoA-I and PEG-HD-Ad-ApoA-I groups, respectively) (**Fig. 23 C**). In HD-Ad-ApoA-I treated mice, LDL-C showed an evident decline starting from the second week of vector administration until the last one. In particular, at 4 weeks, when the total cholesterol levels reached the highest increase, we observed very low concentration of LDL-C compared to that of control mice (148 ± 16 mg/dL vs 399 ± 57 mg/dL). In PEG-HD-Ad-ApoA-I injected mice, the trend of LDL-C was the same than that shown by control mice, throughout the experiment. Also for HDL-C, the basal levels were the same among the 3 groups (114 ± 6 mg/dL, 118 ± 5 mg/dL and 109 ± 8 mg/dL in PBS, HD-Ad-ApoA-I and PEG-HD-Ad-ApoA-I groups, respectively) but, starting from the second week after the injection of HD-Ad-ApoA-I, HDL-C values increased, while LDL-C declined (**Fig. 23 D**). In this group of animals, HDL-C was significantly higher than that in control mice ($p < 0,0001$) until the 12 weeks, reaching plateau already at 4 weeks. Instead, PEG-HD-Ad-ApoA-I treated mice showed, also in HDL-C, the same trend of untreated animals.

7 HD-Ad-ApoA-I treatment prevents aortic atherosclerotic development.

As demonstrated in our experiments, mentioned above, LDLR^{-/-} mice, injected with HD-Ad-ApoA-I, show an improvement in reverse transport of cholesterol, associated with higher levels of HDL-C and consequently lower levels of LDL-C than untreated mice. To check if these changes in the lipidic metabolism have an effect on the atherosclerotic lesion development, we sacrificed animals 12 weeks after vectors injection and dissected out the aortas, from heart to iliac branching. At a macroscopic analysis, fat deposits were observed, as expected, in the intimal

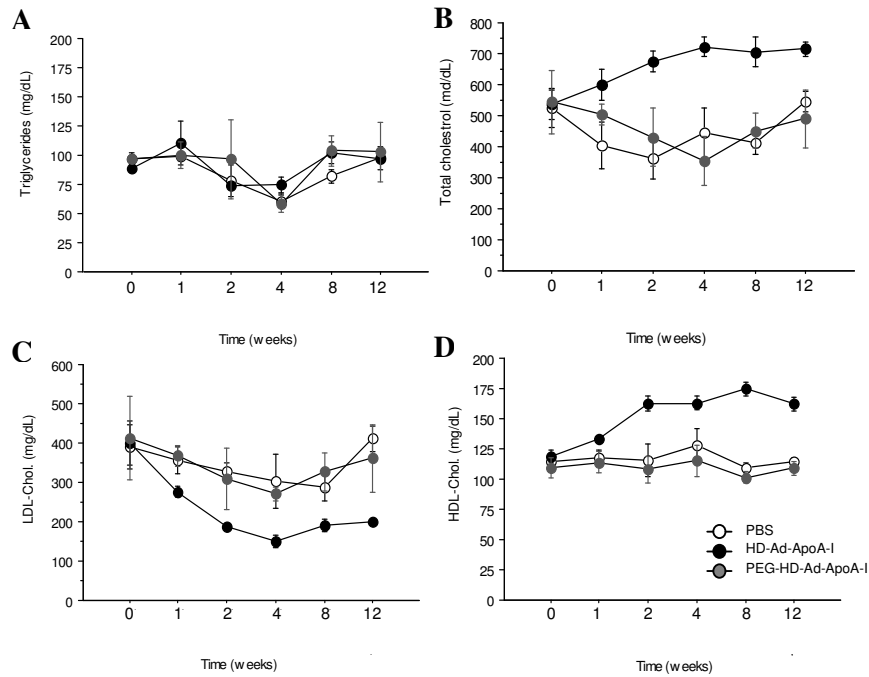


Figure 23. HD-Ad-ApoA-I treatment have a positive effect on metabolism of cholesterol.

LDLR^{-/-} mice were injected systemically with 1×10^{13} vp/kg of HD-Ad-ApoA-I and PEG-HD-Ad-ApoA-I. Mice treated with a same volume of PBS were used as control. 1, 2, 4, 8 and 12 weeks after the treatment, blood samples were collected. Triglycerides (A), total cholesterol (B), LDL-C (C) and HDL-C (D) levels were analysed.

layer of brachiocephalic trunk, left common carotid artery and left subclavian artery, the branches gives off aortic arch (*Fig. 24*). Moreover, other lesions were looked through abdominal aorta, upstream kidney bifurcation. A thorough analysis showed more consistent deposits in mice treated with PBS and PEG-HD-Ad-ApoA-I than that in mice injected with HD-Ad-ApoA-I. Indeed, the first two groups of animals had a greater amount of fats at level of aortic arch than the last group of mice and at abdominal aorta level, in mice administrated with PBS and PEG-HD-Ad-ApoA-I, it was possible observed an occlusion of the artery, associated with a dilatation of the vessel in the point in which fats were deposited. This obstruction was not reported in mice receiving HD-Ad-ApoA-I vector. To quantify the atherosclerotic lesion, directly correlated with fat deposits, an O-Red-Oil staining was carried out on the aortas, opening and cleaning from external fat and leftover tissues. The density of fats, staining in red, was quantified on the area of whole aorta and it was $2 \pm 0,53$, $0,65 \pm 0,3$, $1,9 \pm 0,48$ in mice treated with PBS, HD-Ad-ApoA-I and PEG-HD-Ad-ApoA-I respectively (*Fig. 25*). The reduction in lesion area was significant in animals injected with HD-Ad-ApoA-I compared with the mice receiving PBS and PEG-HD-Ad-ApoA-I ($p < 0,0001$). All the data obtained in mice treated with HD-Ad-ApoA-I, but not with PEG-HD-Ad-ApoA-I, are in accordance with our observations on cholesterol metabolism and correlate with previously experiments (Pastore, 2004) in which an improvement in reverse transport of cholesterol is associated with a decrease in aortic atherosclerotic development.

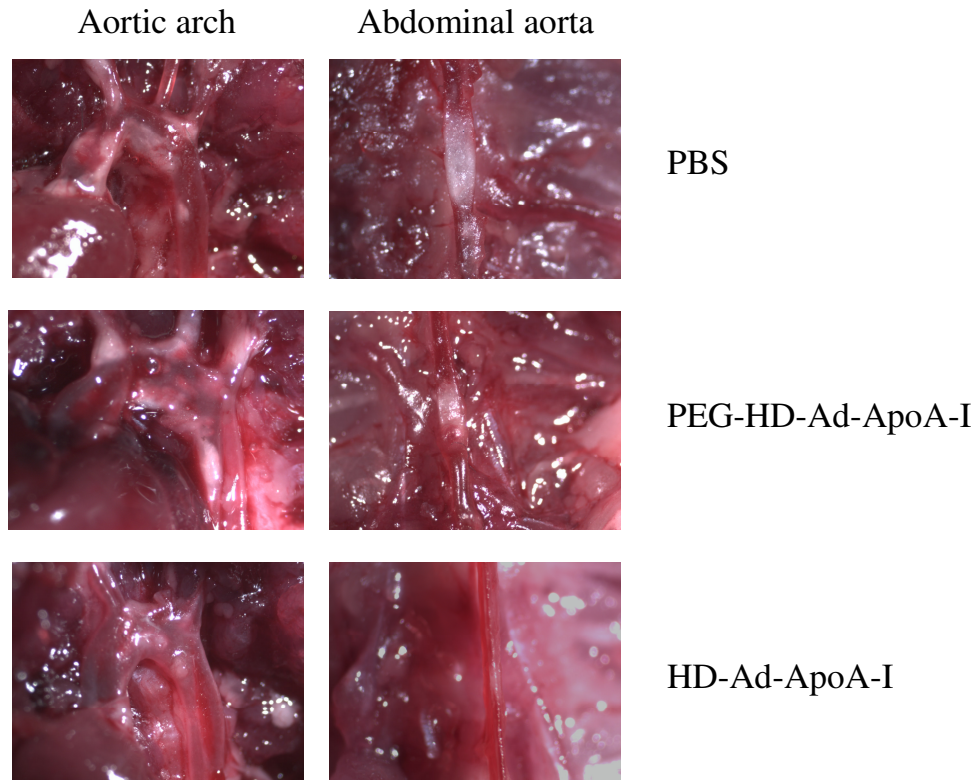


Figure 24. HD-Ad-ApoA-I treatment prevents fat deposits accumulation.

LDLR^{-/-} mice were injected systemically with 1×10^{13} vp/kg of HD-Ad-ApoA-I and PEG-HD-Ad-ApoA-I. Mice treated with a same volume of PBS were used as control. Twelve weeks after the injection, mice were sacrificed and aorta were dissected. Panels show fat deposits in aortic arch and abdominal aorta in treated and untreated mice.

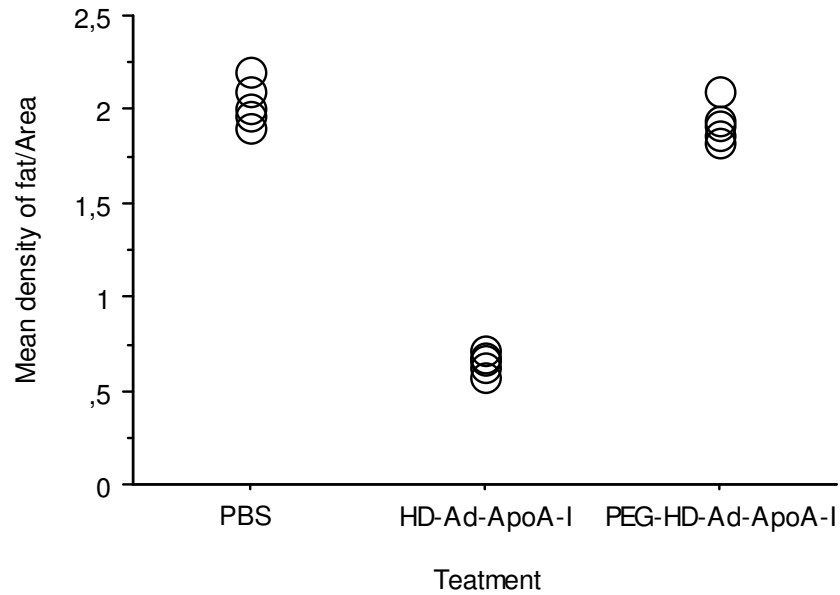


Figure 25. HD-Ad-ApoA-I treatment leads to a decrease in aortic atherosclerotic lesions.

LDLR^{-/-} mice were injected systemically with 1×10^{13} vp/kg of HD-Ad-ApoA-I and PEG-HD-Ad-ApoA-I. Mice treated with a same volume of PBS were used as control. Twelve weeks after the injection, mice were sacrificed and aortas were dissected and stained with O-Red-Oil to identify fats deposits. Red intensity was measured on the area of whole aorta as index of atherosclerotic lesions.

DISCUSSION

Adenovirus mediated gene therapy holds significant potential especially for applications requiring high levels of target tissue transduction and long term expression of transgene. Nevertheless, the clinical translation of adenoviral gene replacement therapy for genetic disease is lagged by vector associated toxicity. Advances in vector production have led to the development of Helper-Dependent adenoviral vectors (HD-Ad) which are characterized by the deletion of all viral coding genes. HD-Ad significantly reduces chronic toxicity which, on the contrary, is strongly induced, in both small and large animal models, by systemic administration of early generation adenoviral vectors. However, even using HD-Ad vectors, innate immune response to adenoviral capsid proteins persists as well as the adaptive immune response to transgene. Together, these two host responses lead to a decrease in the effectiveness of therapeutic index for any particular treatment. Several studies have been carried out in order to reduce the innate immune response to HD-Ad vectors using different approaches such as hydrodynamic injection in mice (Brunetti-Pierri, 2005), balloon occlusion catheter-based method in non human primates (Brunetti-Pierri, 2007) and PEGylation of vectors, whose administration has been performed in mice, in association or not with immunosuppressive drugs (Croyle, 2005; De Geest, 2005). Nevertheless, the molecular pathways involved in the early phase of immune response to adenoviral vectors, are only partially understood.

Therefore, in the first part of this study, we focused our attention in the elucidation of this topic. Previous studies showed that TLR9 (Cerullo, 2007), residing in the endosomal compartment of cells, can be activated by foreign DNA, including the adenoviral genome. The activation of TLR9 leads to an increase in serum levels of several cytokines, suggesting its involvement in the activation of the proinflammatory cytokines occurring after intravenous administration of HD-Ad vectors. Although its significance, TLR9 does not play an important role in the first events involved in innate immune response to adenovirus, owing to its intracellular localization (Cerullo, 2007). This let hypothesize that other TLRs are involved in the host response. To verify this, we first characterized the role of MyD88 in the pathogenesis of the innate immune response that contributes to the *in vivo* HD-Ad toxic reaction following systemic administration. Moreover, we

also identified TLR2 as a major player of the acute inflammatory response. Indeed, PEGylation may mask the interaction between HD-Ad and TLR2, thus explaining a mechanism by which the PEG molecule can protect against the Ad-mediated acute cytokine response.

Regarding to the first point, we clearly showed that MyD88 knockout mice exhibit a 50-70% reduction of pro-inflammatory cytokines production when challenged systemically with high dose of HD-Ad. Since MyD88 is considered a key downstream component in the activation pathways of several TLRs, we have then decided to investigate the role of TLRs expressing on the plasma membrane. In particular, we have studied TLR2 which is known to function as a pattern recognition receptor for several microbial agents, including viruses, and is widely expressed from a variety of cell type, including hepatocytes and Kupffer cells. Moreover, TLR2 molecular pathway converges at activation of MyD88 signaling. As for MyD88^{-/-} mice, TLR2^{-/-} mice, injected with two different doses of HD-Ad vector, have shown, in both dosages, a decrease in proinflammatory cytokines. This drop in the level of cytokines, however, does not depend by a reduced hepatocytes transduction since this last phenomenon occurs at the same extent both in mutant and in wild type mice (C57BL/6). These data highlight an important role for TLR2 as an “early sensor” receptor implied in the activation of innate immune response to HD-Ad vectors. However, both MyD88 and TLR2 knockout mice have not shown a complete abrogation of the toxic response, thus suggesting that other pathways are also involved in the activation of the pro-inflammatory cytokine cascade.

To strengthen the involvement of TLR2 in innate immune response to adenoviral vectors and clarify the mechanism involved in the reduction of toxicity of PEG-HD-Ad, previously shown in several studies, we have treated TLR2^{-/-} mice with a PEGylated vector. TLR2^{-/-} mice exhibited a decrease in the proinflammatory cytokines, compared to control C57BL/6 animals, providing evidence that PEG molecule could mask the viral capsid from the interaction with TLR2. Further experiments are necessary to elucidate whether a direct interaction between TLR2 and viral capsid proteins occurs. Moreover, it remains to be elucidated whether other TLRs are engaged in the response to HD-Ad capsid. However, these

findings significantly contribute to dissect the molecular pathways involved in the innate response to HD-Ad and offer further target molecules for modulating the innate response, hence increasing the safety profile of HD-Ad vectors. Given that many players are involved in the acute toxic reaction to Ad vectors, blocking only one component of this network is unlikely to be beneficial. Therefore, combinatorial therapies to decrease toxicity could be required to increase the maximal tolerated dose and improve the therapeutic window of the therapeutical vector.

Previous studies on toxicity induced by PEG-HD-Ad have been carried out exclusively on C57BL/6 mouse strain, evaluating the effect of the vector injection within 3 days after administration. Moreover, only one transgene (LacZ) has been used in the different studies performed to evaluate the toxicity of HD-Ad. This could turn out as a limitation, not allowing to point out if PEGylation reaction can influence the expression of other transgenes. Therefore, in the second part of this study, we aimed to check whether the use of PEG-HD-Ad vectors can be applied also to pathological animal models. For this reason, we have used a mouse model of atherosclerosis (LDLR^{-/-} mice) which show increased basal levels of LDL-C and a development of atherosclerotic lesion, under a regimen of high cholesterol diet. A previous work on this animal model showed a correction of the pathological phenotype after the injection of HD-Ad-ApoA-I (Belalcazar, 2003). In this study, the retard in atherosclerosis progression and remodeling of the lesions was due to the overexpression of ApoA-I and the consequent increase in reverse transport of cholesterol. In our study, we treated LDLR^{-/-} mice with high doses of HD-Ad-ApoA-I or PEG-HD-Ad-ApoA-I vector and followed, for 12 weeks, the changes in the metabolism of cholesterol, in particular, in the levels of triglycerides, total cholesterol, LDL-C and HDL-C. As a first parameter of investigation, we measured the toxicity of vectors: as in C57BL/6 mice, the PEGylation of vector induced a lower increase in proinflammatory cytokines, compared to mice administered with HD-Ad vector. This data also indicates, for the first time, that the low toxicity due to PEG is independent from transgene used in the therapy. Even if PEG-HD-Ad-ApoA-I displayed low levels of IL-6, the PEGylated vector was not able to induce any effects in blood lipidic pattern.

Indeed, the concentration of total cholesterol, LDL-C and HDL-C in mice receiving PEG-HD-Ad-ApoA-I remained at levels comparable to those displayed by mice administered with PBS. On the other hand, mice treated with HD-Ad-ApoA-I showed significant changes in these parameters. This observation is mirrored by the analysis of fat deposits accumulation at level of aortic arch and abdominal aorta. In fact, untreated and PEG-HD-Ad-ApoA-I mice showed more consistent deposits in comparison to the group injected with HD-Ad-ApoA-I. This data can be explained by a putative different ability of PEG-HD-Ad-ApoA-I and HD-Ad-ApoA-I to infect tissues. In particular, the therapeutic effect of HD-Ad-ApoA-I on atherosclerotic development strongly fit the ability of this vector to infect the mouse endothelium. Indeed, previously work (Gu, 2007) has shown that the expression of human ApoA-I in endothelial cells has a protective role on myocyte injury, suppressing the expression of ICAM-1 on endothelium, thus diminishing neutrophil adherence and transendothelial migration. In our case, it is possible that the binding of PEG to capsid proteins of HD-Ad vectors may hamper the endothelial infection by these vectors, compromising the transgene expression. In a complex pathology model, like our atherosclerotic mouse, a low expression of human ApoA-I in the endothelium would lead to a non-correction of pathological phenotype. On the other hand, higher endothelial expression of human ApoA-I with HD-Ad-ApoA-I would decrease the development of atherosclerotic lesion. In the end, our data clearly show that other factors are implied in the ability of PEGylated vector to revert the pathological phenotype examined, even if PEG-HD-Ad is able to reduce innate immune response and is effective to infect the liver after a systemic administration.

However, in order to confirm our hypothesis, it would be necessary to perform a study of biodistribution of PEG-HD-Ad vectors and analyze the transgene expression profile in different tissues before considering the eventuality to use them in clinical trials for correcting genetic diseases.

REFERENCES

- Akira S (2006) TLR signaling. *Current topics in microbiology and immunology* 311: 1-16.
- Anderson CW, Young ME, Flint SJ (1989) Characterization of the adenovirus 2 virion protein, mu. *Virology* 172(2): 506-512.
- Angeletti PC, Engler JA (1998) Adenovirus preterminal protein binds to the CAD enzyme at active sites of viral DNA replication on the nuclear matrix. *Journal of virology* 72(4): 2896-2904.
- Baker AH, McVey JH, Waddington SN, Di Paolo NC, Shayakhmetov DM (2007) The influence of blood on in vivo adenovirus bio-distribution and transduction. *Mol Ther* 15(8): 1410-1416.
- Balamotis MA, Huang K, Mitani K (2004) Efficient delivery and stable gene expression in a hematopoietic cell line using a chimeric serotype 35 fiber pseudotyped helper-dependent adenoviral vector. *Virology* 324(1): 229-237.
- Belalcazar LM, Merched A, Carr B, Oka K, Chen KH et al. (2003) Long-term stable expression of human apolipoprotein A-I mediated by helper-dependent adenovirus gene transfer inhibits atherosclerosis progression and remodels atherosclerotic plaques in a mouse model of familial hypercholesterolemia. *Circulation* 107(21): 2726-2732.
- Ben-Israel H, Kleinberger T (2002) Adenovirus and cell cycle control. *Front Biosci* 7: d1369-1395.
- Bennett EM, Bennink JR, Yewdell JW, Brodsky FM (1999) Cutting edge: adenovirus E19 has two mechanisms for affecting class I MHC expression. *J Immunol* 162(9): 5049-5052.
- Bergelson JM, Cunningham JA, Droguett G, Kurt-Jones EA, Krithivas A et al. (1997) Isolation of a common receptor for Coxsackie B viruses and adenoviruses 2 and 5. *Science (New York, NY)* 275(5304): 1320-1323.
- Berk AJ (1986) Adenovirus promoters and E1A transactivation. *Annual review of genetics* 20: 45-79.
- Bruder JT, Kovesdi I (1997) Adenovirus infection stimulates the Raf/MAPK signaling pathway and induces interleukin-8 expression. *Journal of virology* 71(1): 398-404.
- Brunetti-Pierrri N, Palmer DJ, Mane V, Finegold M, Beaudet AL et al. (2005) Increased hepatic transduction with reduced systemic dissemination and proinflammatory cytokines following hydrodynamic injection of helper-dependent adenoviral vectors. *Mol Ther* 12(1): 99-106.

- Brunetti-Pierri N, Stapleton GE, Palmer DJ, Zuo Y, Mane VP et al. (2007) Pseudo-hydrodynamic delivery of helper-dependent adenoviral vectors into non-human primates for liver-directed gene therapy. *Mol Ther* 15(4): 732-740.
- Cepko CL, Sharp PA (1983) Analysis of Ad5 hexon and 100K ts mutants using conformation-specific monoclonal antibodies. *Virology* 129(1): 137-154.
- Cerullo V, Seiler MP, Mane V, Brunetti-Pierri N, Clarke C et al. (2007) Toll-like receptor 9 triggers an innate immune response to helper-dependent adenoviral vectors. *Mol Ther* 15(2): 378-385.
- Cotter MJ, Zaiss AK, Muruve DA (2005) Neutrophils interact with adenovirus vectors via Fc receptors and complement receptor 1. *Journal of virology* 79(23): 14622-14631.
- Croyle MA, Yu QC, Wilson JM (2000) Development of a rapid method for the PEGylation of adenoviruses with enhanced transduction and improved stability under harsh storage conditions. *Human gene therapy* 11(12): 1713-1722.
- Croyle MA, Chirmule N, Zhang Y, Wilson JM (2002) PEGylation of E1-deleted adenovirus vectors allows significant gene expression on readministration to liver. *Human gene therapy* 13(15): 1887-1900.
- Croyle MA, Le HT, Linse KD, Cerullo V, Toietta G et al. (2005) PEGylated helper-dependent adenoviral vectors: highly efficient vectors with an enhanced safety profile. *Gene therapy* 12(7): 579-587.
- De Geest B, Snoeys J, Van Linthout S, Lievens J, Collen D (2005) Elimination of innate immune responses and liver inflammation by PEGylation of adenoviral vectors and methylprednisolone. *Human gene therapy* 16(12): 1439-1451.
- Fang B, Eisensmith RC, Wang H, Kay MA, Cross RE et al. (1995) Gene therapy for hemophilia B: host immunosuppression prolongs the therapeutic effect of adenovirus-mediated factor IX expression. *Human gene therapy* 6(8): 1039-1044.
- Fessler SP, Young CS (1999) The role of the L4 33K gene in adenovirus infection. *Virology* 263(2): 507-516.
- Gaggar A, Shayakhmetov DM, Lieber A (2003) CD46 is a cellular receptor for group B adenoviruses. *Nature medicine* 9(11): 1408-1412.
- Graham FL, Smiley J, Russell WC, Nairn R (1977) Characteristics of a human cell line transformed by DNA from human adenovirus type 5. *The Journal of general virology* 36(1): 59-74.

- Gu SS, Shi N, Wu MP (2007) The protective effect of ApolipoproteinA-I on myocardial ischemia-reperfusion injury in rats. *Life sciences* 81(9): 702-709.
- Harlow E, Whyte P, Franza BR, Jr., Schley C (1986) Association of adenovirus early-region 1A proteins with cellular polypeptides. *Molecular and cellular biology* 6(5): 1579-1589.
- Hasson TB, Soloway PD, Ornelles DA, Doerfler W, Shenk T (1989) Adenovirus L1 52- and 55-kilodalton proteins are required for assembly of virions. *Journal of virology* 63(9): 3612-3621.
- He TC, Zhou S, da Costa LT, Yu J, Kinzler KW et al. (1998) A simplified system for generating recombinant adenoviruses. *Proceedings of the National Academy of Sciences of the United States of America* 95(5): 2509-2514.
- Ilan Y (1999) Oral tolerance: a new tool for the treatment of gastrointestinal inflammatory disorders and liver-directed gene therapy. *Canadian journal of gastroenterology = Journal canadien de gastroenterologie* 13(10): 829-835.
- Kafri T, Morgan D, Krahl T, Sarvetnick N, Sherman L et al. (1998) Cellular immune response to adenoviral vector infected cells does not require de novo viral gene expression: implications for gene therapy. *Proceedings of the National Academy of Sciences of the United States of America* 95(19): 11377-11382.
- Kaisho T, Akira S (2006) Toll-like receptor function and signaling. *The Journal of allergy and clinical immunology* 117(5): 979-987; quiz 988.
- Kiang A, Hartman ZC, Everett RS, Serra D, Jiang H et al. (2006) Multiple innate inflammatory responses induced after systemic adenovirus vector delivery depend on a functional complement system. *Mol Ther* 14(4): 588-598.
- Kobayashi K, Oka K, Forte T, Ishida B, Teng B et al. (1996) Reversal of hypercholesterolemia in low density lipoprotein receptor knockout mice by adenovirus-mediated gene transfer of the very low density lipoprotein receptor. *The Journal of biological chemistry* 271(12): 6852-6860.
- Kuriyama S, Tominaga K, Kikukawa M, Tsujimoto T, Nakatani T et al. (1999) Transient cyclophosphamide treatment before intraportal readministration of an adenoviral vector can induce re-expression of the original gene construct in rat liver. *Gene therapy* 6(5): 749-757.
- Leopold PL, Kreitzer G, Miyazawa N, Rempel S, Pfister KK et al. (2000) Dynein- and microtubule-mediated translocation of adenovirus serotype 5 occurs after endosomal lysis. *Human gene therapy* 11(1): 151-165.

- Li E, Stupack D, Bokoch GM, Nemerow GR (1998) Adenovirus endocytosis requires actin cytoskeleton reorganization mediated by Rho family GTPases. *Journal of virology* 72(11): 8806-8812.
- Liu Q, Zaiss AK, Colarusso P, Patel K, Haljan G et al. (2003) The role of capsid-endothelial interactions in the innate immune response to adenovirus vectors. *Human gene therapy* 14(7): 627-643.
- Lochmuller H, Jani A, Huard J, Prescott S, Simoneau M et al. (1994) Emergence of early region 1-containing replication-competent adenovirus in stocks of replication-defective adenovirus recombinants (delta E1 + delta E3) during multiple passages in 293 cells. *Human gene therapy* 5(12): 1485-1491.
- Lukashok SA, Horwitz MS (1998) New perspectives in adenoviruses. *Current clinical topics in infectious diseases* 18: 286-305.
- Matthews DA, Russell WC (1994) Adenovirus protein-protein interactions: hexon and protein VI. *The Journal of general virology* 75 (Pt 12): 3365-3374.
- Matthews DA, Russell WC (1998) Adenovirus core protein V interacts with p32--a protein which is associated with both the mitochondria and the nucleus. *The Journal of general virology* 79 (Pt 7): 1677-1685.
- Morrall N, Parks RJ, Zhou H, Langston C, Schiedner G et al. (1998) High doses of a helper-dependent adenoviral vector yield supraphysiological levels of alpha1-antitrypsin with negligible toxicity. *Human gene therapy* 9(18): 2709-2716.
- Muruve DA, Cotter MJ, Zaiss AK, White LR, Liu Q et al. (2004) Helper-dependent adenovirus vectors elicit intact innate but attenuated adaptive host immune responses in vivo. *Journal of virology* 78(11): 5966-5972.
- Ng P, Parks RJ, Graham FL (2002) Preparation of helper-dependent adenoviral vectors. *Methods in molecular medicine* 69: 371-388.
- Nociari M, Ocheretina O, Schoggins JW, Falck-Pedersen E (2007) Sensing infection by adenovirus: Toll-like receptor-independent viral DNA recognition signals activation of the interferon regulatory factor 3 master regulator. *Journal of virology* 81(8): 4145-4157.
- Nomura S, Merched A, Nour E, Dieker C, Oka K et al. (2004) Low-density lipoprotein receptor gene therapy using helper-dependent adenovirus produces long-term protection against atherosclerosis in a mouse model of familial hypercholesterolemia. *Gene therapy* 11(20): 1540-1548.
- Oka K, Pastore L, Kim IH, Merched A, Nomura S et al. (2001) Long-term stable correction of low-density lipoprotein receptor-deficient mice with a

helper-dependent adenoviral vector expressing the very low-density lipoprotein receptor. *Circulation* 103(9): 1274-1281.

Othman M, Labelle A, Mazzetti I, Elbatarny HS, Lillicrap D (2007) Adenovirus-induced thrombocytopenia: the role of von Willebrand factor and P-selectin in mediating accelerated platelet clearance. *Blood* 109(7): 2832-2839.

Palmer D, Ng P (2003) Improved system for helper-dependent adenoviral vector production. *Mol Ther* 8(5): 846-852.

Parks RJ, Chen L, Anton M, Sankar U, Rudnicki MA et al. (1996) A helper-dependent adenovirus vector system: removal of helper virus by Cre-mediated excision of the viral packaging signal. *Proceedings of the National Academy of Sciences of the United States of America* 93(24): 13565-13570.

Pastore L, Belalcazar LM, Oka K, Cela R, Lee B et al. (2004) Helper-dependent adenoviral vector-mediated long-term expression of human apolipoprotein A-I reduces atherosclerosis in apo E-deficient mice. *Gene* 327(2): 153-160.

Querido E, Blanchette P, Yan Q, Kamura T, Morrison M et al. (2001) Degradation of p53 by adenovirus E4orf6 and E1B55K proteins occurs via a novel mechanism involving a Cullin-containing complex. *Genes & development* 15(23): 3104-3117.

Rekosh DM, Russell WC, Bellet AJ, Robinson AJ (1977) Identification of a protein linked to the ends of adenovirus DNA. *Cell* 11(2): 283-295.

Rowe WP, Huebner RJ, Gilmore LK, Parrott RH, Ward TG (1953) Isolation of a cytopathogenic agent from human adenoids undergoing spontaneous degeneration in tissue culture. *Proceedings of the Society for Experimental Biology and Medicine Society for Experimental Biology and Medicine* (New York, NY) 84(3): 570-573.

Schiedner G, Morral N, Parks RJ, Wu Y, Koopmans SC et al. (1998) Genomic DNA transfer with a high-capacity adenovirus vector results in improved in vivo gene expression and decreased toxicity. *Nature genetics* 18(2): 180-183.

Stewart PL, Fuller SD, Burnett RM (1993) Difference imaging of adenovirus: bridging the resolution gap between X-ray crystallography and electron microscopy. *The EMBO journal* 12(7): 2589-2599.

Stewart PL, Chiu CY, Huang S, Muir T, Zhao Y et al. (1997) Cryo-EM visualization of an exposed RGD epitope on adenovirus that escapes antibody neutralization. *The EMBO journal* 16(6): 1189-1198.

- Sundararajan R, Cuconati A, Nelson D, White E (2001) Tumor necrosis factor- α induces Bax-Bak interaction and apoptosis, which is inhibited by adenovirus E1B 19K. *The Journal of biological chemistry* 276(48): 45120-45127.
- Tangirala RK, Tsukamoto K, Chun SH, Usher D, Pure E et al. (1999) Regression of atherosclerosis induced by liver-directed gene transfer of apolipoprotein A-I in mice. *Circulation* 100(17): 1816-1822.
- Tollefson AE, Scaria A, Hermiston TW, Ryerse JS, Wold LJ et al. (1996) The adenovirus death protein (E3-11.6K) is required at very late stages of infection for efficient cell lysis and release of adenovirus from infected cells. *Journal of virology* 70(4): 2296-2306.
- Walter J, You Q, Hagstrom JN, Sands M, High KA (1996) Successful expression of human factor IX following repeat administration of adenoviral vector in mice. *Proceedings of the National Academy of Sciences of the United States of America* 93(7): 3056-3061.
- Webster A, Russell WC, Kemp GD (1989) Characterization of the adenovirus proteinase: development and use of a specific peptide assay. *The Journal of general virology* 70 (Pt 12): 3215-3223.
- Wickham TJ, Mathias P, Cheresch DA, Nemerow GR (1993) Integrins $\alpha v \beta 3$ and $\alpha v \beta 5$ promote adenovirus internalization but not virus attachment. *Cell* 73(2): 309-319.
- Yang Y, Nunes FA, Berencsi K, Gonczol E, Engelhardt JF et al. (1994) Inactivation of E2a in recombinant adenoviruses improves the prospect for gene therapy in cystic fibrosis. *Nature genetics* 7(3): 362-369.
- Zhang W, Imperiale MJ (2003) Requirement of the adenovirus IVa2 protein for virus assembly. *Journal of virology* 77(6): 3586-3594.

INDEX

INTRODUCTION.....	ERRORE. IL SEGNALIBRO NON È DEFINITO.
1. THE STRUCTURE OF ADENOVIRUSES.....	ERRORE. IL SEGNALIBRO NON È DEFINITO.
2. VIRAL LIFE CYCLE.....	ERRORE. IL SEGNALIBRO NON È DEFINITO.
2.1 EARLY EVENTS IN ADENOVIRUS INFECTION ..	ERRORE. IL SEGNALIBRO NON È DEFINITO.
2.2 EARLY GENE AND DNA REPLICATION	ERRORE. IL SEGNALIBRO NON È DEFINITO.
2.3 LATE GENE EXPRESSION AND VIRAL ASSEMBLY.....	- 8 -
3. ADENOVIRUSES AS VECTORS.....	ERRORE. IL SEGNALIBRO NON È DEFINITO.
3.1 FIRST AND SECOND GENERATION OF ADENOVIRAL VECTORS	ERRORE. IL SEGNALIBRO NON È DEFINITO.
3.2 HELPER-DEPENDENT VECTORS	ERRORE. IL SEGNALIBRO NON È DEFINITO.
3.3 IMMUNE RESPONSE TO AD BASED VECTORS .	ERRORE. IL SEGNALIBRO NON È DEFINITO.
3.4 PEGYLATION AND PRELIMINARY DATA.....	ERRORE. IL SEGNALIBRO NON È DEFINITO.
4. ATHEROSCLEROSIS.....	ERRORE. IL SEGNALIBRO NON È DEFINITO.
4.1 LIPOPROTEIN METABOLISM	ERRORE. IL SEGNALIBRO NON È DEFINITO.
4.2 PLAQUE PROGRESSION IN ATHEROSCLEROSIS	ERRORE. IL SEGNALIBRO NON È DEFINITO.
4.3 ANIMAL MODELS FOR ATHEROSCLEROSIS AND PRELIMINARY DATA	ERRORE. IL SEGNALIBRO NON È DEFINITO.

MATERIALS AND METHODS.....	ERRORE. IL SEGNALIBRO NON È DEFINITO.
-----------------------------------	--

1. PRODUCTION OF HELPER-DEPENDENT ADENOVIRAL VECTORS	ERRORE. IL SEGNALIBRO NON È DEFINITO.
2. PEGYLATION OF HD-AD VECTORS.....	ERRORE. IL SEGNALIBRO NON È DEFINITO.

3. CHARACTERIZATION OF PEGYLATED HD-AD VECTORS.....	ERRORE. IL SEGNALIBRO NON È DEFINITO.
4. IMMUNOTURDIMETRIC ASSAY.....	- 37 -
5. ANIMAL STUDIES.....	- 38 -
6. EVALUATION OF TOXICITY.....	- 39 -
7. X-GAL STAINING AND B-GAL ENZYME ASSAY.....	- 39 -
8. LIPIDS MEASUREMENT.....	- 39 -
9. DISSECTION OF AORTAS AND QUANTIZATION OF ATHEROSCLEROTIC LESIONS.....	- 40 -
10. STATISTICAL ANALYSIS.....	- 40 -

RESULTS.....ERRORE. IL SEGNALIBRO NON È DEFINITO.

1. PRODUCTION AND CHARACTERIZATION OF HD-AD VECTORS	ERRORE. IL SEGNALIBRO NON È DEFINITO.
2. ROLE OF MYD88 IN THE ACUTE INFLAMMATORY RESPONSE TRIGGERED BY SYSTEMIC HD-AD ADMINISTRATION.....	ERRORE. IL SEGNALIBRO NON È DEFINITO.
3. TLR2 DEFICIENCY ATTENUATES THE INNATE IMMUNE RESPONSE TO HD-AD VECTORS <i>IN VIVO</i>	- 50 -
4. PEGYLATION MASKS THE INTERACTION BETWEEN HD-AD AND TLR2.....	- 53 -
5. TOXICITY OF HD-AD-APOA-I AND PEG-HD-AD-APOA-I IN A MOUSE MODEL OF ATHEROSCLEROSIS.....	- 54 -
6. HD-AD-APOA-I, BUT NO PEG-HD-AD-APOA-I, INDUCES EFFECTS IN BLOOD LIPIDIC PATTERN.....	- 56 -
7. HD-AD-APOA-I TREATMENT PREVENTS AORTIC ATHEROSCLEROTIC DEVELOPMENT.....	- 58 -

DISCUSSION.....ERRORE. IL SEGNALIBRO NON È DEFINITO.

BIBLIOGRAPHY.....ERRORE. IL SEGNALIBRO NON È DEFINITO.

